

1 **Aquatic ecosystem changes in a global biodiversity hotspot: evidence from the Albertine**
2 **Rift, central Africa**

3
4 ¹McGlynn, G., ²Lejju, J., ³Dalton, C., ⁴Mooney, S.D., ⁵Rose, N.L., ⁶Tompkins, A.M.,
5 ⁷Bannister, W., ⁷Tan, Z. D., ⁴Zheng, X., ⁸Rühland, K. and ^{7,9*}Taylor, D
6

7 ¹Department of Geography, School of Natural Sciences, Trinity College Dublin, Dublin 2,
8 Ireland.

9 ²Department of Biology, Mbarara University of Science and Technology, P.O. Box 1410,
10 Mbarara, Uganda

11 ³Department of Geography, Mary Immaculate College, University of Limerick, Limerick,
12 Ireland.

13 ⁴School of Biological, Earth and Environmental Sciences, The University of New South
14 Wales, Sydney 2052, NSW

15 ⁵Environmental Change Research Centre, Department of Geography, University College
16 London, London, WC1E 6BT, UK

17 ⁶Abdus Salam International Centre for Theoretical Physics, Trieste, Italy

18 ⁷Department of Geography, National University of Singapore, Singapore 117570

19 ⁸Department of Biology, Queen's University, Kingston, Ontario, Canada, K7L 3N6.
20

21 ⁹Current address: School of Geography, University of Melbourne, Carlton, Victoria,
22 Australia, 3053.

23

24 ***Corresponding author:** David Taylor; Tel: +65 6516 7394; Fax: +65 6777 3091; email:

25 geodmt@nus.edu.sg

26

27

28 **Type of paper:** Research Paper

29 **Abstract**

30 **Aim**

31 Determine the extent to which remote, high-altitude (Afroalpine) aquatic ecosystems in
32 tropical Africa have been impacted by global and regional-scale environmental change
33 processes.

34 **Location**

35 Two volcanic crater lakes (Bisoke and Muhavura) in the Afroalpine zone, Albertine (Western)
36 Rift, central Africa.

37 **Methods**

38 Sediment cores were collected from Bisoke and Muhavura lakes and dated using radiometric
39 techniques. A range of sediment based-proxies was extracted from the cores and quantified.
40 Sedimentary data were subjected to statistical analyses that contributed to the identification of
41 influential environmental variables and their effects on diatom assemblages, the determination
42 of variations in spatial beta diversity and estimates of the rate of compositional turnover over
43 the last c. 1200 years.

44 **Results**

45 Sediments from the two sites provide evidence of the sensitivity of remote, Afroalpine aquatic
46 ecosystems to perturbation. Climate variability has been a major driver of ecological change,
47 particularly at Bisoke Lake, throughout the c. 1200 year-long record, while Muhavura Lake
48 has been directly impacted by and recovered from at least one volcanic eruption during this
49 time. The effects of climatic warming from the mid- to late-19th century and especially from
50 the late-20th century, possibly accentuated by atmospheric deposition-driven nutrient
51 enrichment, appear increasingly in lockstep. Effects include changes in diatom community
52 composition, increased productivity and compositional turnover, and biotic homogenisation
53 (reduced spatial beta diversity) between the two sites.

54 **Main conclusions**

55 The two Afroalpine sites record changes in atmospheric conditions and their effects on diatom
56 assemblage composition, particularly over the last c. 150 years. Drivers of these changes have
57 the potential to disrupt ecosystems at lower altitudes in the Albertine Rift, including
58 biodiverse areas of forest, and across tropical Africa more widely.

59

60 **KEYWORDS:** Afroalpine, atmospheric deposition, biotic homogenisation, climate change,
61 eutrophication, pollution

62 **1. INTRODUCTION**

63 Global warming poses a significant threat to mountainous regions (Steinbauer et al., 2018).
64 More rapid rates of temperature increase at higher altitudes when compared with lower
65 elevations (MRI, 2015), together with substantial losses in range area as climates warm, pose
66 significant risks to montane taxa (Moritz & Agudo, 2013). Although alpine ecosystems
67 globally are at risk, those located in the tropics may be particularly sensitive and vulnerable to
68 climate change (Zimmer et al., 2018).

69
70 Climate change is just one of several pressures faced by montane areas at low latitudes.
71 Productivity in high-altitude ecosystems is typically strongly nutrient limited (Cárate-
72 Tandalla, Camenzind, Leuschner, & Homeier, 2018) and is thus sensitive to changes in the
73 availability of nutrients (Gütlein et al., 2017). One means through which nutrients might
74 become more available in remote high-altitude locations is through increased atmospheric
75 depositions of, for example, nitrogen (N) arising from human-induced disruptions to the
76 global N cycle. Disruptions to the global N cycle can occur via the conversion of largely
77 unreactive molecular N to a reactive state (reactive N [Nr]) that is available to biota before
78 being returned to the atmosphere by microbial denitrification. The industrial-scale conversion
79 of N into ammonia (NH₃)-based fertilisers has severely disrupted the global N cycle and led
80 to dramatically increased environmental levels of Nr (Fowler et al., 2013), as have
81 anthropogenic emissions of N₂O. Biomass burning is another, often overlooked, potential
82 source of Nr (Benedict et al., 2017).

83
84 Despite their vulnerability, tropical high-altitude ecosystems are among the most poorly
85 studied on Earth (Buytaert, Cuesta-Camacho, & Tobón, 2011). Consequently, little
86 knowledge exists of the actual extent to which montane taxa are being impacted by global-

87 and regional-scale drivers of change. One exception is the discovery that recent increases in
88 air temperature may have driven ecological changes in tropical Andean lakes (Michelutti et
89 al., 2015), although Fritz, Benito & Steinitz-Kannan (2019) suggest that the effects may be
90 less evident in larger lakes, particularly when viewed in the context of sedimentary evidence
91 spanning a millennium or more. Lakes can be sentinels of changing atmospheric conditions
92 and their effects (Catalan et al., 2013), especially when located in small, isolated catchments
93 above the treeline and with minimal direct anthropogenic disturbance. Even relatively small
94 changes in temperature and nutrient availability can have profound impacts on key physical
95 and biological processes that go on to be recorded in lake sediments. As Michelutti et al.
96 (2015) demonstrate, lake sediment records can be particularly valuable in the absence of, or as
97 a complement to, direct measurements of environmental changes and their effects.

98
99 Here we present new sedimentary evidence of aquatic ecological changes over the last c. 1200
100 years from the Afroalpine zone in the highly biodiverse Albertine, or Western, Rift that forms
101 the western perimeter to equatorial eastern Africa. The Albertine Rift supports one of 35
102 global biodiversity hotspots (Mittermeier, Turner, Larsen, Brooks, & Gascon, 2011) and has
103 become an important focus for biodiversity conservation efforts (Plumptre et al., 2007). Aside
104 from climate change (Ponce-Reyes et al., 2017), high levels of species diversity and
105 endemism are directly threatened by human activity, with human population densities more
106 than 300% greater than the mean for sub-Saharan Africa (Burgess et al., 2007). More
107 insidious processes, such as variations in land values, declining agricultural productivity and
108 political insecurity, also pose a significant threat to biodiversity in the region (Ayebare,
109 Plumptre, Kujirakwinja, & Segan, 2018; Hochleithner, 2017; Salerno et al., 2018). To date,
110 however, there is little if any empirical evidence of biotic responses to current environmental

111 changes at high-altitude in the Albertine Rift, or indeed cool- and low-nutrient adapted taxa
112 associated with the Afroalpine belt more widely.

113

114 This paper provides evidence of the extent to which climate change and possibly also
115 pollution from atmospheric deposition, are impacting aquatic biota in two remote, high-
116 altitude crater lakes in the Virunga volcanoes, Albertine Rift, within the context of the last
117 1200 years or so of ecological variability. The remains of diatoms (Bacillariophyceae)
118 preserved in sediment are a particular focus; diatoms have been widely used to track changes
119 in water quality and as indicators of biological condition more broadly (Battarbee et al., 2001;
120 Hausmann, Charles, Gerritsen & Belton, 2016). The sediment records obtained provide a
121 basis for assessing biodiversity trends over an expanded period of time that extends to before
122 the onset of the current period of significant, widespread human impacts, or the proposed
123 Anthropocene Epoch (McGill, Dornelas, Gotelli & Magurran, 2015; Steffen, Grinevald,
124 Crutzen, & McNeil, 2011). In addition to being important in their own right, the two high-
125 elevation lakes may also be viewed as sentinels of broader-scale, atmosphere-transmitted
126 ecological pressures in the Albertine Rift.

127

128 **2. MATERIALS AND METHODS**

129 **2.1 Study area and sites**

130 The Virunga volcanoes, rising steeply from a relatively undulating volcanic plain to
131 elevations well over 4000m above sea level (asl), form part of the Virunga Conservation Area
132 (Fig. 1). Located close to the Equator, variations in day length and monthly mean
133 temperatures are relatively minor. Significant seasonal variations in rainfall exist, reflecting
134 the annual migration of the tropical rain belt and the position and strength of the Congo Air
135 Boundary. The main wet season usually occurs during April-June, when airflows from the

136 Atlantic Ocean predominate, and is followed by a second, shorter, wet season in November-
137 December, during which the Indian Ocean has a greater influence. Temperature decreases
138 with altitude, while rainfall levels peak at about 2300-3000m and low clouds and mist are
139 common occurrences on mountain summits (Hedberg, 1964; Spinage, 1972). At the highest
140 elevation strong diurnal variations in temperature occur, with day-night differences dampened
141 at times by relatively high humidity.

142

143 Vegetation on the volcanoes has a marked altitudinal zonation in response to altitude-related
144 changes in climate conditions. Lower montane forest characterises slopes up to an altitude of
145 c. 2500m asl, and likely extended over much of the volcanic plain prior to the onset of Late
146 Iron Age clearances in the region around 1000 years ago (Taylor, 1990). Bamboo thickets are
147 present above the lower montane forest, while Ericaceous vegetation occurs between c.
148 3000m asl and 3600m asl. Afroalpine vegetation is found on the highest mountains above c.
149 3600m asl with more sheltered locations hosting the most mesic, shrubby vegetation cover.
150 Short alpine grassland and areas of bare rock are found on the highest, exposed slopes.

151

152 The two study sites are crater lakes at the summits of Mount (Mt.) Bisoke and Mt. Muhavura,
153 hereafter referred to as, respectively, Bisoke Lake and Muhavura Lake. Both are located
154 above the treeline in the Afroalpine zone in small, clearly defined and topographically-closed
155 catchments that are largely undisturbed by the direct effects of human activity. Bisoke Lake
156 has a much greater volume and is set within a far larger crater than Muhavura Lake (Table 1).
157 Moreover, Muhavura Lake (4127 m asl) has an elevation around 400m greater than Bisoke
158 Lake. Vegetation in the crater on Mt. Bisoke is characterised by a dense cover of shrubby
159 Afroalpine vegetation, notably giant lobelia (e.g. *Lobelia stuhlmannii* Schweinf. ex Stuhlmann
160 and *L. wollastonii* Baker f.) and groundsels (*Dendrosenecio johnstonii* (Oliv.) B.Nord). Alpine

161 grasses (members of the Pooideae), sparse giant lobelia and groundsels and areas of bare rock
162 characterise the geomorphologically more subdued crater at the summit of Mt. Muhavura.

163

164 **2.2 Field sampling**

165 Sediment core BIS3, 110cm long, was extracted from the deepest part of Bisoke Lake in 2010
166 using a tapper corer (Chambers & Cameron, 2001). BIS3 was sampled in the field in 1cm-
167 thick slices. The total depth of the longest of several sequences of sediments extracted from
168 Muhavura Lake in 2008 was 247cm. This paper focuses on the uppermost 120cm of this
169 sequence, comprising a short 37cm-long core (MUH4) obtained using a Renberg gravity corer
170 and the uppermost part of core MUH2. Core MUH2 was extracted in 1m-long sections using
171 a modified Livingstone piston corer, with each section off-set to provide a c. 50cm overlap
172 between sections. Both BIS3 and MUH4 captured the sediment-water interface. Unfortunately
173 a 13cm-long section of sediment between the base of MUH4 at 37cm and the top of MUH2 at
174 50cm below the surface was not collected. Core sections comprising MUH2 were packaged
175 and shipped entire for subsampling in 1cm-thick slices in the laboratory. Overlaps between
176 sections were verified, post collection, using sedimentary data (McGlynn, Mooney, & Taylor,
177 2013). All cores and core samples were stored at 2 °C prior to laboratory analyses.

178

179 **2.3 Sedimentary analyses**

180 **2.3.1 Chronological control and estimated sediment accumulation rates (SAR)**

181 Chronological control and estimated SAR were established using radiometric dating
182 techniques and BACON, software that enables the systematic establishment of sediment age-
183 depth relationships using a Bayesian, hierarchical model with autoregressive gamma
184 processes (Blaauw & Christen, 2011). Down-profile variations in ^{210}Pb and application of the
185 Constant Rate of Supply (CRS) model (Appleby & Oldfield, 1978) were used to date the

186 uppermost parts of the sediment sequences from both sites. Measurements of ^{137}Cs activity,
187 and what is assumed to be the 1963 CE peak (9.5cm in BIS3 and 15.5cm in MUH4), provided
188 independent validation of the CRS model. Changes in abundances of the isotopes were
189 established for MUH4 and the upper part of BIS3 by direct gamma assay using an ORTEC
190 HPGe GWL series well-type coaxial low background intrinsic germanium detector (Appleby,
191 2001). Thirteen AMS ^{14}C dates were obtained on plant macrofossil fragments (initially
192 identified as terrestrial in origin) extracted from BIS3 and MUH2. All conventional ^{14}C dates,
193 expressed along with their 2σ errors, were calibrated using INTCAL13 (Reimer et al., 2013).
194 Bayesian models can take into account prior knowledge. This allowed the age-depth model
195 for Muhavura Lake to take account of a 10cm thick tephra-rich layer (80-90cm) in MUH2,
196 which was regarded as having been deposited within a single year. Thus sediment deposited
197 between 80 and 90 cm in MUH2 was given the same age.

198

199 **2.3.2 Sediment proxies**

200 Percentage organic matter was measured via loss-on-ignition on 1cm-thick, contiguous
201 sediment slices for BIS3, and on 1cm-thick sediment slices with at least a 2cm resolution for
202 MUH4/MUH2 (Heiri, Lotter, & Lemcke, 2001). Spheroidal carbonaceous particles (SCP)
203 were enumerated in 16 samples from BIS3 in accordance with Rose (1994, 2008), and are
204 expressed as fluxes ($n \text{ particles cm}^{-2} \text{ yr}^{-1}$). SCP, a component of black carbon, are released
205 during the industrial-scale combustion of coal and fuel oil (Rose, Harlock & Appleby, 1999).
206 The atmospheric deposition of SCP is generally assumed to be coherent over relatively small
207 areas (Rose, Juggins, Watt, & Battarbee, 1994) and has been used as a proxy of acidifying
208 substances associated with emissions from power stations and other power-intensive
209 industries dependent upon coal and fuel oils (Heard et al., 2014). Samples from
210 MUH4/MUH2 were not subjected to SCP analysis.

211

212 Percentage total organic carbon (%TOC), percentage total nitrogen (%TN) and ratios of
213 carbon ($\delta^{13}\text{C}$) and nitrogen ($\delta^{15}\text{N}$) stable isotopes provide an indication of the source of
214 organic matter fraction of sediments (Meyers, 2003; Talbot, 2001) and were determined for
215 55 and 29 samples from, respectively, BIS3 and MUH4/MUH2. Samples were analysed on
216 either a Finnegan Delta plus XP gas source mass spectrometer (BIS3 and MUH4) or a
217 Thermo Deltaplus Continuous Flow Isotope Ratio Mass Spectrometer (MUH2). Atomic C/N
218 ratios were calculated based on %TOC and %TN. $\delta^{13}\text{C}$ values were calculated to the VPDB
219 scale using a within-run laboratory standard, while $\delta^{15}\text{N}$ values were calculated relative to
220 atmospheric N.

221

222 Diatom remains were concentrated in sediment samples in accordance with standard
223 procedures (Battarbee et al., 2001); a total of 33 samples from BIS3 and 30 from
224 MUH4/MUH2 were analysed. A minimum of 400 valves was counted in each sample
225 (Battarbee et al., 2001). Diatoms were identified primarily in accordance with Gasse (1986),
226 Krammer & Lange-Bertalot (1986-1991), Krammer (1992), Lange-Bertalot & Moser (1994),
227 Cocquyt (1998) and Cocquyt & Jahn (2007) and are expressed in percentage terms (sum =
228 total number of valves counted in each sample). Total diatom counts are also expressed as
229 flux (number of frustules $\text{cm}^{-2} \text{year}^{-1}$)

230

231 Preparation of pollen preserved in sediment samples, here used as a guide to changes in local
232 and regional vegetation, followed Bennett & Willis (2001). Pollen data from a total of 28
233 samples were determined; 16 from BIS3 and 12 from MUH4/MUH2. At least 500 pollen
234 grains and spores were identified for each sediment sample and expressed as percentages
235 (sum = total pollen and spores, excluding damaged grains). Sediment samples were analysed

236 for charcoal content, a proxy for vegetation fires. Fluxes in macro-charcoal (area of fragments
237 $>250\mu\text{m}$, $\text{mm}^2 \text{ cm}^{-2} \text{ yr}^{-1}$), which may largely reflect local burning (Conedera et al., 2009),
238 were quantified in 52 and 21 sediment samples from, respectively, BIS3 and MUH2/MUH4,
239 using a modification of the wet-sieving method (Mooney & Tinner, 2011). Variations in
240 micro-charcoal (area of fragments $<140\mu\text{m}$, $\text{cm}^2 \text{ cm}^{-3}$), generally assumed to include material
241 of long-distance origin and therefore to represent the burning of biomass over a wide area,
242 were also determined on 12 samples from MUH4/MUH2 using a modification of the size-
243 classing technique (Waddington, 1969).

244

245 **2.4 Numerical analysis**

246 Diatom-based biostratigraphic zones were identified by cluster analysis using constrained
247 incremental sum of squares (CONISS) in the programme Tilia v 2.0-41 (Grimm, 1987) with
248 chord distance (Cavalli-Sforza & Edwards, 1967) as the dissimilarity measure, and a broken-
249 stick model to determine the optimum number of diatom zones (Bennett, 1996). Diatom
250 remains were also used to infer past variations in pH (diatom-inferred pH, DI-pH) at both
251 sites using a transfer function approach (Birks, 1995). A classic weighted averaging model
252 with tolerance down weighting and inverse deshrinking was deployed. Since no diatom
253 training set specific to Afroalpine lakes is available, the European Diatom Database (EDDI;
254 <http://craticula.ncl.ac.uk/eddi>) was used as a basis for DI-pH estimations. EDDI includes
255 alpine lakes in Europe, and sub-alpine lakes in eastern Africa, including medium altitude
256 crater lakes in western Uganda (Mills & Ryves, 2012). Reconstructions of pH were performed
257 using the software ERNIE (Environmental Reconstruction using the EDDI diatom database)
258 v. 1.2. The use of transfer functions to infer individual environmental variables from among a
259 complex of interacting forces has increasingly been questioned (Davidson, Bennion, Reid,

260 Sayer & Whitmore, 2018). Here DI-pH is viewed cautiously in the absence of monitoring data
261 and as one of several components of reconstructed variations in water quality.

262

263 Multivariate ordination was carried out on the diatom and selected environmental proxy data
264 (% organic matter, %TN, %TOC, atomic C/N and $\delta^{13}\text{C}$, $\delta^{15}\text{N}$) (Constrained Correspondence
265 Analysis, CCA) and solely on diatom data (Principal components analysis, PCA) from both
266 sites using CANOCO 4.5 (ter Braak and Šmilauer, 2002). Only taxa that attained an
267 abundance of 1% or greater in at least one sample were included in the CONISS, CCA and
268 PCA analyses. Data were not transformed prior to analysis. CCA allows the fitting of possible
269 gradients of environmental influences to ecological data (ter Braak, 1986), while PCA
270 provides a means of summarising major trends in data. Because of the fragmented nature of
271 meteorological records in the region and difficulties in accurately matching-up those data that
272 are available with sedimentary evidence, variations in temperature and precipitation were not
273 included in the analysis as potential environmental influences. All of the environmental
274 variables included in the first CCA run scored Variation Inflation Factor (VIF) values > 20,
275 with %N and %C scoring highest in, respectively, BIS3 and MUH4/MUH2. A second run of
276 CCA with %N (BIS3) and %C (MUH4/MUH2) excluded resulted in VIF values < 20 for both
277 sites.

278

279 CANOCO 4.5 was also used to carry out Detrended Canonical Correspondence Analysis
280 (DCCA) on diatom data from both sites, including rarely occurring taxa. Diatom data were
281 square root transformed. DCCA can be used to generate an estimate of total compositional
282 turnover, measured as beta diversity and scaled in standard deviation (SD) units (Birks, 2007),
283 where a SD of 4.0 represents a 100% turnover of taxa (Legendre & Birks, 2010; ter Braak &
284 Prentice, 1988). Differences in diatom compositional turnover (i.e. beta diversity) at the two

285 sites were estimated by DCCA within the entire stratigraphical record, and for intervals
286 representing time periods before and after the mid-19th century (Birks, 2007; Smol et al.,
287 2005). The latter division, which roughly marks the boundary between the pre-industrial and
288 the industrial ages (Waters, Zalasiewicz, Williams, Ellis & Snelling, 2014) was included to
289 determine the effects, if any, of anthropogenic activity. Aquatic acidification and
290 eutrophication become widespread in northern Europe and North America from the mid-19th
291 century (Battarbee et al. 2011; Wilkinson, Poirier, Head, Sayer & Tibby, 2014), while
292 climatic warming and its effects on lake stratification and productivity over the last 150 years
293 or so are recorded in Lake Tanganyika sediments (Cohen et al., 2016). In addition, variations
294 in spatial beta diversity, or the degree of homogenisation, were determined based on a
295 Sørensen distance metric and presence/absence data using the R package BETAPART and the
296 function beta.multi (Anderson, 2006; Baselga & Orme, 2002), and following the method
297 outlined in Wengrat et al. (2018). This involved first dividing the diatom data into pairs of
298 samples, one from each site, in which the estimated age range of one sample overlapped with
299 the other in the same pair. The latter requirement resulted in some data not being included in
300 the analysis and a total of 16 pairs of samples (Table S1). A simple linear regression was used
301 to estimate the relationship between estimated age of the sample pairs and their corresponding
302 Sørensen distance metric using EXCEL.

303

304 **3. RESULTS**

305 **3.1. Chronology**

306 Results of all AMS ¹⁴C, ²¹⁰Pb and ¹³⁷Cs analyses, the latter including the 1963 CE ¹³⁷Cs peak,
307 were used as input to the age-depth modelling and are summarised in Tables S2 and S3 and
308 Fig. S1. The seven AMS ¹⁴C dates from Muhavura were reported in McGlynn et al. (2013),
309 while the six from BIS3 have not previously been published. Results from the age-depth

310 modelling are shown in Fig. S2. For the remainder of this paper, only the mean of the
311 estimated range of ages for the sample depth, rounded to the nearest multiple of five, is
312 quoted. Full information on the actual estimated ages and errors (2σ) of all sample depths, at
313 1cm resolution, is provided for both BIS3 and MUH4/MUH2 in Table S4. Accordingly, the
314 estimated age of the base of BIS3 is 610 CE, while 120cm in MUH4/MUH2 corresponds to
315 805 CE. The gap in the sediment record between MUH4 and MUH2 equates to c. 200 years,
316 from 1650 CE to 1860 CE. Sediment accumulation rates increase in both sequences from the
317 beginning of the 20th century and particularly from the 1960s in BIS3 (Fig. S1).

318

319 **3.2 Sedimentary and numerical analyses**

320 Down-core variations in sedimentary data for BIS3 and the uppermost 120cm of sediment in
321 MUH4/MUH2 are summarised in Fig. 2. Fig. 3 illustrates changes in relatively abundant and
322 ecologically-significant diatom taxa referred to below.

323

324 Sediment cores from both lakes were largely dark-coloured, organic, fine grained with
325 occasional inclusions of plant macrofossils. Their largely organic nature is supported in the
326 laboratory measurements; levels of organic matter are generally above 40%: BIS3 mean =
327 $48.5 \pm 9.6\%$, range = 20.2 to 65.3%; MUH4/MUH2 mean = $50.9 \pm 13.0\%$, range = 8.4 to 84.8
328 %. Levels of organic matter in BIS3 are noticeably higher, in general, in the uppermost part of
329 the core (above c. 1860 AD) than lower in the sequence. Lowest organic matter values at both
330 sites are from periods of accumulation of relatively inorganic sediment, dated 1530 CE to
331 1815 CE (Bisoke Lake) and 1170 CE to 1195 CE (Muhavura Lake) - the latter included a
332 brown-coloured, tephra-rich layer. The tephra had a sugary textured appearance, either a
333 blocky or flatter sharp/angular morphology and contained numerous micro-inclusions.

334

335 Mean atomic C/N ratios for BIS3 and MUH4/MUH2 are, respectively, 15.5 ± 2.5 , ranging
336 from 10.6 to 20.0, and 17.9 ± 1.1 , ranging from 16.0 to 20.1. Levels of $\delta^{13}\text{C}$ vary throughout
337 both sequences, although no trends are evident, with less variability in the data for BIS3
338 compared with the generally less depleted levels for MUH4/MUH2; BIS3 mean = $-25.0 \pm$
339 0.3‰ , range = -25.7 to -24.3‰ : MUH4/MUH2 mean = $-21.0 \pm 1.16\text{‰}$, range = -23.5 to $-$
340 19‰ . Values of $\delta^{15}\text{N}$ are generally a little more enriched in BIS3 than in MUH4/MUH2;
341 BIS3 mean = $4.2 \pm 0.5\text{‰}$, range = 3.2 to 5.3‰: MUH4/MUH2 mean = $2.3 \pm 0.7\text{‰}$, range =
342 0.5 to 3.3‰. They also gradually increase up-core at both sites, and particularly from 1890
343 CE in BIS3 ($\delta^{15}\text{N}$ values show a similar trend in MUH4/MUH2). In both cases, $\delta^{15}\text{N}$
344 enrichment is particularly conspicuous from the 1960s to the present, where BIS3 mean = 5.0
345 $\pm 0.3\text{‰}$ (based on five measurements, and representing a c. 20% increase over the overall
346 mean) and MUH4/MUH2 mean = $2.9 \pm 0.2\text{‰}$ (based on nine measurements, and representing
347 a c. 25% increase over the overall mean). SCP were not enumerated in any of the samples
348 analysed from before 1985 CE in BIS3, after which they increase rapidly in the overlying five
349 samples to peak at $169 \text{ particles cm}^{-2} \text{ yr}^{-1}$ at 2005 CE, before declining slightly again at the
350 surface.

351

352 Diatom remains are well-preserved and abundant throughout both BIS3 and MUH2/MUH4. A
353 total of 59 diatom taxa were enumerated in sediment samples from BIS3, with CONISS
354 identifying zone boundaries at 1460 CE (BS1-BS2) and 1860 CE (BS2-BS3). Zone BS3 was
355 further subdivided into two sub-zones (BS3a and BS3b), with the boundary dated 1985 CE.
356 For MUH4/MUH2, 52 taxa were enumerated. Benthic diatoms, such as several *Eunotia* spp.,
357 are much more prominent throughout MUH4/MUH2 when compared with BIS3. CONISS
358 identified three zones in the diatom record, with boundaries at 1880 CE (MU1-MU2) and
359 1990 CE (MU2-MU3). Both BIS3 and MUH4/MUH2 record substantial changes in diatoms

360 over the last 150 years or so, particularly from the mid 1980s to the present. PCA axes 1 and 2
361 sample scores and DI-pH values also exhibit sharp changes in the late 19th century. PCA axes
362 1 and 2 sample scores in MUH4/MUH2 also exhibit an abrupt oscillation around 1170-1180
363 CE, coincident with the aforementioned brown-coloured tephra-rich layer, a peak in macro-
364 charcoal flux, and relatively low $\delta^{13}\text{C}$ and C/N values, ranging from -1.38 to -0.39.

365

366 Remains of *Aulacoseira alpigena* (Grunow) Krammer, *Brachysira brebissonii* R. Ross,
367 *Frustulia rhomboides* (Ehrenberg) De Toni and *Eunotia* spp are relatively abundant
368 throughout zone BS1 in BIS3. *B. brebissonii* is the most common taxon in zone MU1 in
369 MUH4/MUH2, along with the benthic species *Pinnularia biceps* Greg and several small
370 *Eunotia* species. Planktonic *Cyclotella ocellata* Pantocsek is not present in shallow Muhavura
371 Lake prior to 1890 CE, and thereafter only sporadically and in low abundances (<1%) when it
372 does occur. The taxon is, however, virtually omnipresent throughout BIS3, and initially
373 increases in abundance in zone BS1 between 850 and 1150 CE. Marked changes in diatom
374 composition occur across the BS1-BS2 zone boundary that are not evident in the diatom data
375 in MUH4/MUH2, where the sampling resolution in this part of the sequence is relatively
376 coarse; both *Stauroforma exiguiformis* (Lange-Bertalot) Flower, V.J. Jones & Round and
377 *Nitzschia paleacea* Grunow becomes more abundant, while *A. alpigena* and *B. brebissonii*
378 both decline. Overall diatom productivity in BS2 increases by c 50% across the BS1-BS2
379 boundary, but remains relatively low.

380

381 Several abrupt changes in diatoms occur across the BS2/BS3a boundary, dated 1860 CE. *S.*
382 *exiguiformis* declines, while *F. rhomboides* and *B. brebissonii* show an initial increase in
383 BS3a, and then a decline in BS3b. *N. paleacea* and *Gomphonema parvulum* (Kützing)
384 disappear completely at the beginning of BS3a, and do not reappear. The abundances of

385 *Luticola mutica* (Kützing) D.G.Mann and *Diadesmis contenta* (Grunow ex Van Heurck)
386 D.G.Mann increase in BS3a and still further in BS3b, the latter along with a second rise in *C.*
387 *ocellata*, while overall diatom productivity shows a major increase from 1980 CE.

388

389 Zone MU2, beginning 1880 CE, is characterised by increased diatom flux, continued relative
390 abundance of *B. brebissonii*, increases in several *Eunotia* species and in *F. rhomboides* and
391 the first appearance of *G. parvulum*. The most marked change in diatoms in MUH4/MUH2
392 occurs across the MU2-MU3 zone boundary, dated 1990 CE, with an abrupt increase in *G.*
393 *parvulum*, and a relative decline in most other taxa. Diatom accumulation rates remain
394 relatively high throughout MU3.

395

396 More than 90 pollen and spore types were enumerated in BIS3 and MUH4/MUH2. Pollen
397 data from the latter are described in full in McGlynn et al. (2013). The most substantial
398 change in vegetation evident in the MUH4/MUH2 part of the record occurred at 1010 CE and
399 comprises a decline in pollen from montane forest taxa. An increased abundance of micro-
400 charcoal also occurs around the same time. The pollen record in BIS3 indicates similar
401 changes in vegetation and fire activity more-or-less contemporaneously, from around 940 CE.
402 BIS3 also records reduced abundance of pollen from some montane forest taxa during the
403 period 1400 to 1760 CE, and concomitant increases in pollen indicating more open vegetation
404 (notably Poaceae and *Dodonaea*). A peak in macro-charcoal flux around 1540 CE indicates
405 burning of vegetation, possibly close to the lake. Further reductions in forest cover are evident
406 in BIS3 over the last 150 years or so, while being more muted in MUH4/MUH2. Increased
407 biomass burning in the region is also evident from the early 1900s, according to a steep rise in
408 abundance of micro-charcoal in MUH4/MUH2. Evidence of sporadic, localised burning in the
409 1900s also exists, however, in the form of isolated peaks in macro-charcoal flux.

410

411 According to results of CCA (Fig. 4, Table S5), $\delta^{15}\text{N}$ and the atomic C/N ratio are the most
412 influential of the selected environmental variables considered. When applied to the complete
413 sets of diatom data, DCCA generated SD scores of 0.54 for BIS3 (33 samples, 640 CE to
414 2010 CE, Fig. 2a) and 1.16 for MUH4/MUH2 (30 samples, 885 CE to 2005 CE, Fig. 2b). A
415 comparison of diatom compositional turnover between pre and post-industrial (~1850 CE)
416 assemblages yielded DCCA gradient lengths of 0.63 SD (20 samples) and 0.68 SD (9
417 samples) for BIS3, respectively. A similar comparison for MUH4/MUH2 yielded DCCA
418 gradient lengths of 1.14 SD for pre-industrial assemblages (20 samples) and 0.86 SD for post-
419 industrial assemblages (10 samples). Sørensen distance metrics decline over time ($R^2 =$
420 0.7072 , $p < 0.001$), indicating that diatom flora at the two lakes are becoming increasing
421 similar (more homogenous) (Table S6). A step change (fall) in Sørensen distance metrics is
422 evident between samples dating to before (7 pairs, mean = 0.52) and those dating to after (9
423 pairs, mean = 0.39) the mid-19th century.

424

425 **4. DISCUSSION**

426 Atomic C/N ratios and $\delta^{13}\text{C}$ values indicate a mixed plant source for the organic fraction of
427 sediments accumulating at both Bisoke and Muhavura lakes, with algae, which are relatively
428 N-enriched compared with more woody aquatic macrophytes and terrestrial plants, generally
429 more prominent contributors to organic matter in BIS3 than MUH4/MUH2 (Meyers &
430 Lallier-Vergès, 1999). Overall, diatom assemblages from the two sites indicate the
431 maintenance of slightly acidic, low conductivity, oligotrophic conditions throughout the last c
432 1200 years (Holmgren, Ljung & Björck, 2012; Kilroy, Biggs, Vyverman, & Broady, 2006;
433 Soeprobowati, Suedy, Hadiyanto, Luis & Gell, 2018). That said, sedimentary sequences from
434 both Bisoke and Muhavura lakes record variations in aquatic conditions and their potential

435 drivers that have important implications for biodiversity conservation, including the
436 protection of remote sites and their biota.

437

438 Benthic diatoms are relatively prominent in MU1, and indeed throughout much of
439 MUH4/MUH2, which is in keeping with the much shallower depth of Muhavura Lake. Two
440 excursions in diatom assemblages are evident during the early part of the sedimentary record.
441 The first, 850 CE to 1150 CE, consists of an increased relative abundance of *Cyclotella*
442 *ocellata* in Bisoke Lake but not in the much shallower Muhavura Lake. Increases in the
443 relative abundance of small planktonic, cyclotelloid taxa, such as *C. ocellata*, at the expense
444 of small, benthic fragilarioid taxa and larger-celled diatom taxa have been widely linked to
445 recent warming-induced, enhanced thermal stability and attendant changes in resource
446 availability in deep alpine lakes (Rühland, Paterson & Smol, 2008, 2015; Michelutti et al.,
447 2015; Saros, Northington, Anderson, & Anderson, 2016; Yan et al., 2018). Small cyclotelloid
448 taxa have a high surface area to volume ratio that results in lower sinking rates (Ptacnik, Diehl
449 & Berger, 2003), greater efficiency in nutrient uptake and light harvesting (Litchman,
450 Klausmeier, Miller, Schofield & Falkowski, 2006) and, under ideal conditions, are often
451 capable of prolific reproduction (Jewson 1992), providing them with a competitive advantage
452 during prolonged periods of stratification (Winder and Hunter 2008; Yang, Stenger-Kovács,
453 Padisák, & Pettersson, 2016). Increased abundances of *C. ocellata* in BS1 could thus reflect
454 the effects of warmer temperatures associated with the Medieval Warm Period (MWP), which
455 was a period of widely experienced warming and other climate-related anomalies in the
456 region from about 950 CE to 1250 CE (Mann et al., 2009), including aridity (Alin & Cohen,
457 2003; Verschuren, Laird & Cumming, 2000). Hypothesized increased stability during the
458 MVP, however, does not appear to have resulted in meromixis-induced, increased
459 preservation of organic matter. The very shallow depth of Muhavura Lake and a greater

460 propensity of mixing of the water column explains the absence of a peak in *C. ocellata* from
461 this site.
462
463 The second excursion is dated c. 1180 CE at Muhavura Lake and is characterised by the
464 presence of a 10cm-thick tephra-rich deposit, abrupt oscillations in PCA axes 1 and 2 sample
465 scores, highly variable rates of diatom flux, large peak in macro-charcoal flux, dip in the
466 proportion of pollen from montane forest taxa, e.g. *Podocarpus*, and relatively depleted $\delta^{13}\text{C}$
467 values, including the lowest measurement (-23.54‰) for the entire sequence. Collectively the
468 data represent the effects of volcanic activity and deposition of a thick, tephra-rich layer in the
469 crater at the summit of Muhavura, including vegetation fires. Deposition of tephra appeared to
470 have little or no long-term impact on diatom assemblages at Muhavura Lake, based on
471 similarities in composition of sediment samples that bracket the tephra-rich layer. The tephra
472 is not evident in sediments recovered from Bisoke Lake. A brown-coloured tephra with a
473 similar morphology to that recovered from Muhavura Lake was, however, recorded at c.
474 1150-1180 CE in a well-dated, 8m-long core of peat sediment from the crater swamp at the
475 summit of Mt. Gahinga, fewer than 5km to the west of Mt. Muhavura, but only in much
476 smaller amounts (<5% concentration). Several peaks in macro-charcoal flux clustered around
477 1200 CE (McGlynn et al., 2013) suggest that vegetation fires could have extended to Mt.
478 Gahinga. The distribution of the tephra could reflect prevailing wind patterns at the time of
479 eruption, which resulted in transportation of the majority of the volcanic debris to the east and
480 south, rather than to the west. Lake Kivu to the south has a rich record of volcanic activity, in
481 the form of thick layers of tephra that suggest an interval of around 500 years between major
482 eruptions of Virunga volcanoes over the last c. 12,000 years (Wood & Scholz, 2017).
483

484 A change in conditions in Bisoke Lake is dated 1460 CE to 1860 CE (diatom zone BS2). The
485 same period is not well covered in the sedimentary record from Muhavura Lake as it partially
486 coincides with the gap in sediment between 1650 CE to 1860 CE. BS2 is characterised by
487 relatively low diatom productivity together with increased PCA 1 axis sample scores and
488 contributions of terrestrial plant material (based on relatively depleted $\delta^{13}\text{C}$ and enhanced C/N
489 data) and inorganic matter to sediments. An increased relative abundance of *Stauroforma*
490 *exiguiformis* and *Nitzschia paleacea*, and declines in the planktonic taxa *Aulacoseira alpigena*
491 and *C. ocellata*, also characterise the zone. *S. exiguiformis* and *N. paleacea* are both benthic,
492 periphytic taxa, while *A. alpigena*, is tolerant of low-light conditions often associated with
493 deep water (Dalton et al., 2018). A fall in water level in Bisoke Lake, resulting in an
494 expansion of littoral and benthic habitats, is indicated, and may have been linked to a period
495 of climatic aridity in the region associated with the main phase of the Little Ice Age (LIA).
496 This commenced in Africa from around 1500 CE (Nash et al., 2016), and was associated with
497 reduced rainfall and lower lake levels throughout western parts of eastern Africa (Mills,
498 Ryves, Anderson, Bryant & Tyler, 2014; Russell, Verschuren & Eggermont, 2007). Increased
499 aridity may have arisen from a change in location and/or a weakening of convergence
500 associated with the Congo Air Boundary (Nash et al., 2016). Climatically drier conditions
501 from around the beginning of the 16th century have been suggested as a driver of changes in
502 the pattern of human settlement and land use in what is now central and western Uganda
503 (Taylor, Marchant & Robertshaw, 1999; Taylor, Robertshaw & Marchant, 2000).

504

505 Some coherence in timing of variations in diatom remains is evident at the two sites from the
506 mid to late 19th century, marked by the BS2-BS3a (1860 CE) and MU1/MU2 (1880 CE)
507 zone boundaries, and from the late 1980s. Substantial changes in PCA axis 1 sample scores
508 during the mid- to late-19th century track the most pronounced diatom assemblage shifts

509 expressed in the sedimentary records of both lakes. A marked decline in the relative
510 abundance of *S. exiguiformis* from 1860 CE suggests a deepening of Bisoke Lake, which
511 accords with evidence from the region for generally increased rainfall, punctuated with
512 occasional, prolonged droughts, from the late 19th century into the early 20th century (Nash
513 et al., 2016). In addition to an increase in precipitation, an increase in the relative abundance
514 of *C. ocellata* provides evidence of recent climatic warming from c. 1900 CE. This is
515 consistent with findings from Lake Tanganyika (Cohen et al. 2016; Tierney et al., 2010). The
516 effects of warming are less evident in the sediments from Muhavura Lake, where in addition
517 to a continued predominance of *Brachysira brebissonii* and other benthic taxa indicative of
518 slightly acidic waters, *Frustulia rhomboides* increases in abundance and *Gomphonema*
519 *parvulum* makes its first appearance. Both *F. rhomboides* and *G. parvulum* are cited as
520 tolerant of nutrient enrichment (Abarca, Jahn, Zimmermann & Enke, 2014; Bellinger,
521 Cocquyt & O'Reilly, 2006; Montoya & Aguirre-Ramírez, 2013). Warmer conditions and a
522 greater availability of nutrients may have brought about an increase in diatom productivity at
523 Bisoke Lake that along with reduced decomposition, owing to a strengthening of stratification
524 (Littke, 1985), could explain an increased contribution of organic matter to sediments from c.
525 1860 AD. Changes in pollen and micro-charcoal recorded at the two sites indicate a reduction
526 in extent of montane forest at lower elevations and an increase in vegetation fires in the
527 region.

528

529 Climate warming, possibly in tandem with increases in nutrient availability, appears to be the
530 main driver of changes in the composition of diatom taxa in the late 1980s, highlighted by the
531 BS3a-BS3b sub-zone (1985 CE) and MU2-MU3 zone (1990 CE) boundaries, with neither site
532 showing evidence of the effects of a continent-wide reduction in rainfall from the 1980s
533 (Nicholson, Funk & Fink, 2018). The abundances of *C. ocellata*, *Diadesmis contenta* and

534 *Luticola mutica* increase in the uppermost part of the sediment sequence from Bisoke Lake,
535 while at Muhavura Lake *G. parvulum* rises to prominence. Diatom flux, while remaining high
536 at both sites, increases at Bisoke Lake. As with *G. parvulum*, increases in abundances of *D.*
537 *contenta* and *L. mutica* and relatively high diatom productivity and increased rate of sediment
538 accumulation could represent responses to increased nutrient availability. *D. contenta*,
539 characteristic of good water quality in general, is tolerant of low levels of pollution and has
540 been recorded in mesotrophic to eutrophic waters in Brazil (Bere & Tundisi, 2011), while *L.*
541 *mutica* is regarded as indicative of elevated nutrient levels (Gell, Sluiter, & Fluin, 2002).

542

543 Meteorological data, although scarce and often highly discontinuous when available, support
544 recent warming in the region. The closest meteorological station to Bisoke and Muhavura
545 lakes is located at Kabale, Uganda, around 30km to the east and c.1900m asl. Data from
546 Kabale show a trend of increasing mean annual temperatures since the 1960s-1970s. A
547 longer, more complete record from the meteorological station at Entebbe, even farther to the
548 east in central Uganda, reveals an increase in mean annual temperatures of around 0.8-1.0 °C
549 since the 1930s. Recent warming in the Albertine Rift is also evident in satellite-derived
550 proxy data from lakes Albert, Rukwa and Tanganyika, indicating a 0.2 to 0.6 °C decade⁻¹
551 increase in temperature of surface waters between 1985 and 2005 (O'Reilly et al., 2015), and
552 in ERA-Interim and ERA-5 reanalysis data centred upon the Virunga volcanoes (Fig. 5).

553

554 Increases in aquatic productivity over the last 100 years or so, and particularly from the mid
555 1970s, are also evident at Lake Bujuku, 3960m asl on Mt. Rwenzori, also part of the Albertine
556 Rift (Panizzo et al., 2008). Nitrogen can play an important role in limiting primary
557 productivity in lakes in the tropics (Abell, Özkundakci, Hamilton, & Jones, 2012), and
558 increasingly enriched $\delta^{15}\text{N}$ values, evident at both Bisoke and Muhavura lakes in the 20th

559 century, and particularly from the 1960s, may represent an increased availability of Nr and
560 consequent relaxation of N-limitations on productivity. Such a scenario is supported by the
561 results of CCA, which identified $\delta^{15}\text{N}$ as an important environmental influence over diatom
562 variations at the two sites, particularly Bisoke Lake. This coherence is at variance with
563 sediment records from some lakes in temperate latitudes, however, which show recent
564 declines in $\delta^{15}\text{N}$ values (Holtgrieve et al., 2011). They are, however, in agreement with
565 enriched $\delta^{15}\text{N}$ values in recently deposited sediments from Lake Wandakara, western Uganda
566 (Russell et al., 2009).

567

568 Contrasting trends in $\delta^{15}\text{N}$ values between Bisoke and Muhavura lakes and lakes in more
569 temperate latitudes could reflect differences in the main sources of N. Hu, Anderson, Yang &
570 McGowan (2014) describe four main pathways through which nutrient enrichment of remote,
571 alpine lakes can occur. Of these, and given their isolated location and the very small size of
572 the catchments relative to lake surface area, enhanced, direct atmospheric deposition of Nr on
573 the lake surface is the most likely cause of $\delta^{15}\text{N}$ enrichment in Bisoke and Muhavura lakes.
574 The presence of SCP in sediments from Bisoke Lake from the mid-1980s is evidence of the
575 importance of both long-distance transport and atmospheric deposition at these remote,
576 mountain-top sites, with the nearest sources potentially several thousand km away. Moreover,
577 SCP accumulation has been linked to eutrophication at a remote lake caused by N deposition
578 from fossil-fuel sources (Pla, Monteith, Flower & Rose, 2009). Biomass burning in the region
579 is, however, perhaps the most obvious source of atmospheric depositions of Nr at Bisoke and
580 Muhavura lakes, in addition to fragments of charcoal. Vegetation fires occur annually on the
581 African continent (van der Werf et al., 2017), and are an important source of atmospheric N,
582 which dominates the N cycle in tropical Africa (Bauters et al., 2018; Galy-Lacaux & Delon,
583 2014). Biomass burning in the region has a long history (Jolly et al., 1997; Taylor, 1990),

584 with sedimentary data from mid-altitude western Uganda indicating a sustained increase in
585 vegetation fires from the mid-20th century (Colombaroli, Ssemmanda, Gelorini & Verschuren,
586 2014). Evidence from Muhavura Lake, and from the northern part of Lake Tanganyika
587 (Cohen et al., 2005), places the onset of the most recent period of increased burning in the
588 region even earlier, to the late 19th/early 20th centuries. The increasingly enhanced $\delta^{15}\text{N}$ values
589 towards the top of the sediment records from Bisoke and Muhavura lakes also implicate
590 increased biomass burning as an important source. Emissions from highly productive
591 agriculture, characterised by high stocking densities and the use of large quantities of
592 fertiliser, and from the combustion of fossil fuel – two other potential sources – tend to be
593 associated with relatively depleted levels of $\delta^{15}\text{N}$ when compared with those from biomass
594 burning (Felix, Elliott, Gish, McConnell, & Shaw 2013; Felix, Elliott, & Shaw, 2012;
595 Kawashima & Kurahashi, 2011; Wang et al., 2017).

596

597 Major ecological changes are evident at both Bisoke and Muhavura lakes throughout the last
598 c. 1200 years, and appear increasingly in lockstep from the mid 19th century and especially
599 from the 1980s. Climate change has been and remains an important driver of variations in
600 aquatic ecological conditions at Bisoke Lake in particular, perhaps because the higher
601 elevation and much smaller size of Muhavura Lake have resulted in shorter-term (e.g. diurnal)
602 and extreme episodic (e.g. volcanic activity) processes having a much greater influence on
603 aquatic biota than climate pressures developing over a longer duration. The sedimentary
604 evidence also suggests nutrient enrichment at both sites, and possibly also variations in pH.
605 The release of CO_2 along with other magmatic gases directly into the water column together
606 with the occurrence of products of weathering of volcanic material may have been local
607 sources of acidification pressures (Balagizi et al., 2015; Pérez et al., 2011), in addition to
608 atmospheric depositions of acidifying material originating in far more distant locations

609

610 According to the results of DCCA, ecological changes at Bisoke Lake include an acceleration
611 in the rate of compositional turnover in diatom assemblages over the last c. 150 years that is
612 less evident at Muhavura Lake. Results from Bisoke Lake are thus in keeping with increased
613 diatom turnover rates reported for the same period for arctic and alpine lakes in the Northern
614 Hemisphere, with Smol et al. (2005) attributing increased turnover primarily to climate
615 warming, while Hobbs et al. (2010) propose increased deposition of Nr as a possible,
616 additional, contributing factor. Furthermore, the distinctiveness of diatom flora at Bisoke and
617 Muhavura lakes also appears to have reduced over time, experiencing a stepped fall when
618 compared with conditions pre mid-19th century. Reduced spatial beta diversity is an
619 increasing concern at present (Dornelas et al., 2014), and has been linked to both climate
620 change and nutrient enrichment (Monchamp et al., 2018; Wengrat et al., 2018; Zwiener, Lira-
621 Noriega, Grady, Padial & Vitule, 2018).

622

623 The ecological effects of recent warming, possibly in combination with increased availability
624 of nutrients, presented here have coincided with a ramping-up of conservation efforts in the
625 Virunga volcanoes (Robbins et al., 2011). The effects are unlikely to be restricted to Bisoke
626 and Muhavura lakes, given the potential geographic scope of the drivers. Future research will
627 determine the extent to which anthropogenic climate change and other large-area effects of
628 transboundary pollution are impacting the Albertine Rift, including biodiverse-rich areas of
629 forest at lower altitudes, and indeed tropical Africa more widely.

630

631 **ACKNOWLEDGEMENTS**

632 This research was funded by the Irish Research Council, with additional support provided by
633 the National Geographic Society (research grant ‘Climate change, fire and ecosystem

634 response on the Virunga volcanoes’) and Mary Immaculate College, University of Limerick.
635 Research permission was provided by the Uganda Wildlife Authority (UWA/TDO/33/02), the
636 Ugandan National Council for Science and Technology (NS196) and the Rwanda
637 Development Board. Thanks to Elaine Doyle (charcoal) and Patrick Carroll (pollen) for
638 assistance with laboratory analysis of core BIS3, to Poonam Saksena-Taylor for assistance
639 with figures, and to Prosper Uwingeli, Glenn Bush, May Murungi, Stephen Taylor and Yonah
640 Okoth for help in the field.
641

Table 1: Geographical, physical and limnological information on Bisoke and Muhavura lakes (crater lakes at the summits of Mt Bisoke and Mt Muhavura). *asl = above sea level. +Note that in the absence of lake water quality monitoring data, information from surface sediment measurements is referred to. **Diatom-inferred value ~ see text for further information.

| Lake | Latitude/ Longitude | Altitude (m asl*) | Lake surface area (m ²) | Max depth (m) | Lake catchment area (m ²) | Lake area:catchment area ratio | pH ($\pm 2\sigma$) ^{+,**} | Atomic C:N ratio ⁺ | $\delta^{13}\text{C}$ (‰) ⁺ | $\delta^{15}\text{N}$ (‰) ⁺ |
|----------|--------------------------------|-------------------------|---|---------------------|---|--------------------------------------|---|-------------------------------------|---|---|
| Bisoke | 29° 29' 12" E/ 1° 27' 40" S | 3711 | 70695 | 21 | 124,315 | 0.57 | 5.83 (0.43) | 16.72 | -24.86 | +5.26 |
| Muhavura | 29° 40' 42" E/ 1° 23' 0" S | 4127 | 491 | 1.6 | 604 | 0.81 | 6.54 (0.45) | 15.43 | -20.08 | +3.31 |

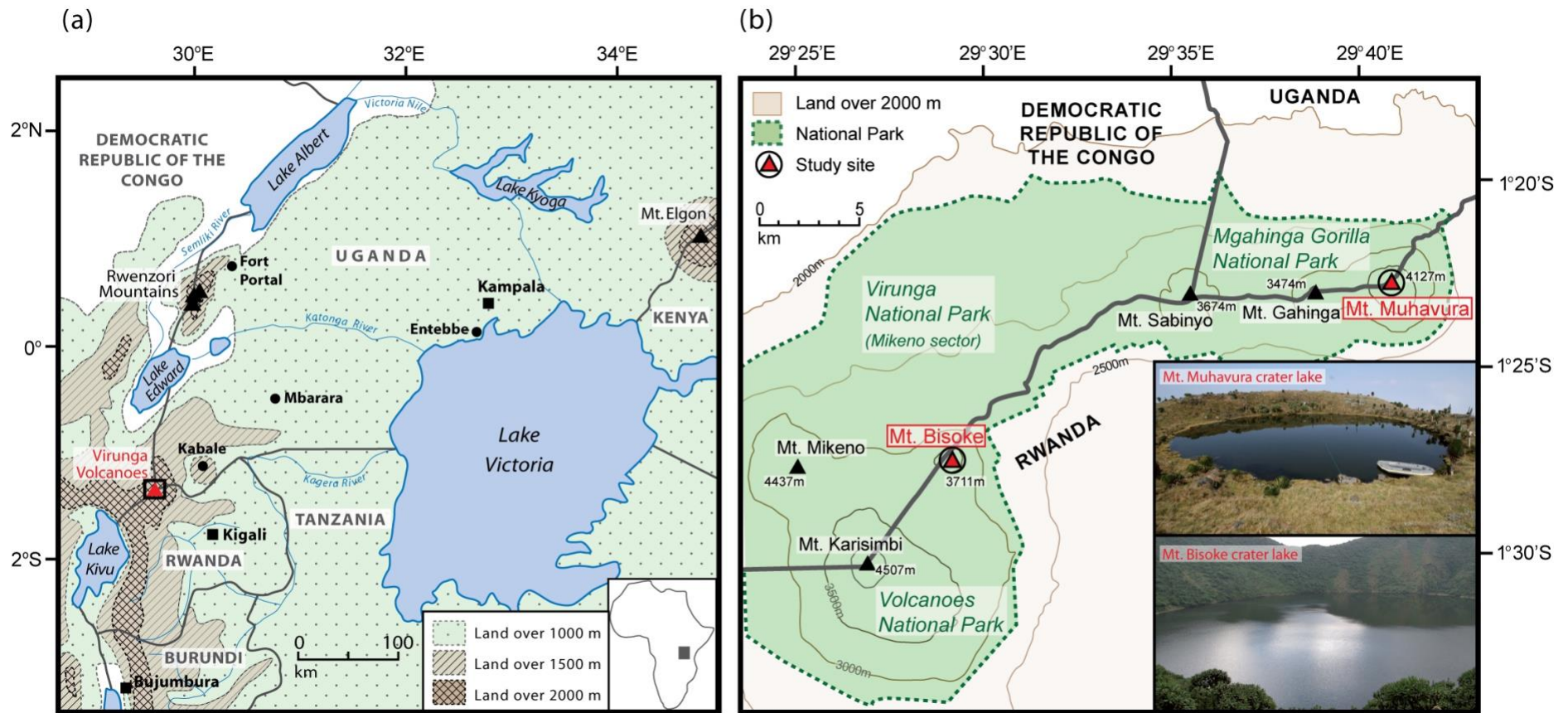
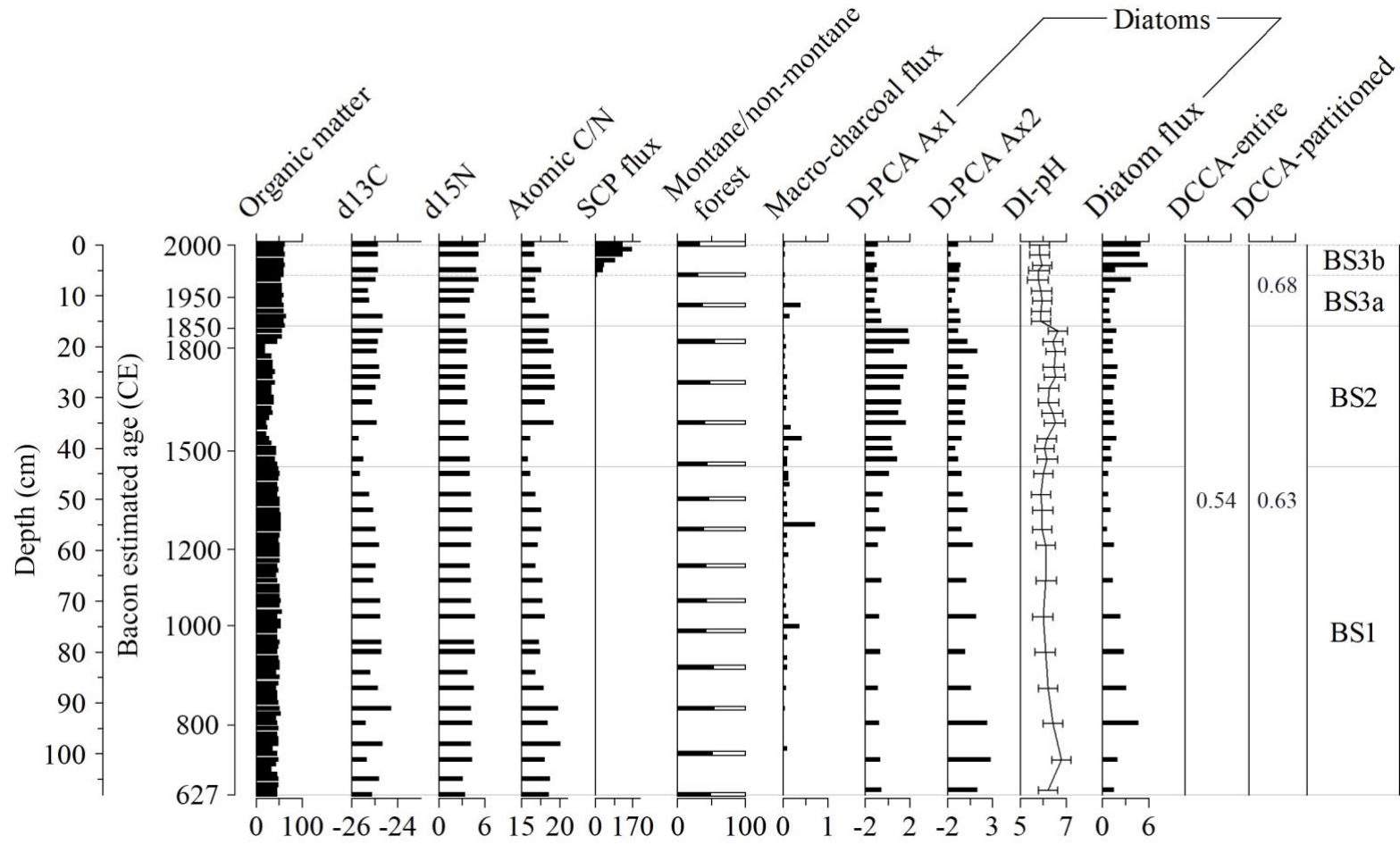


Figure 1: Location of the Virunga volcanoes in the Albertine Rift, which also accommodates the lakes of (from south to north) Tanganyika, Kivu, Edward and Albert, and forms the western boundary of eastern Africa (a). Location of Bisoke and Muhavura crater lakes on Mt Bisoke and Mt Muhavura within the Virunga Conservation Area, which comprises three national parks. All altitudes shown are in metres above sea level (m asl). The two photographs show the sample sites on Mt Muhavura (upper photograph) and Mt Bisoke (lower photograph). Note the very different sizes and vegetation cover in the two craters. Sediment cores were collected during several periods of fieldwork in 2008 (Mt Muhavura) and 2010 (Mt Bisoke).

a)



b)

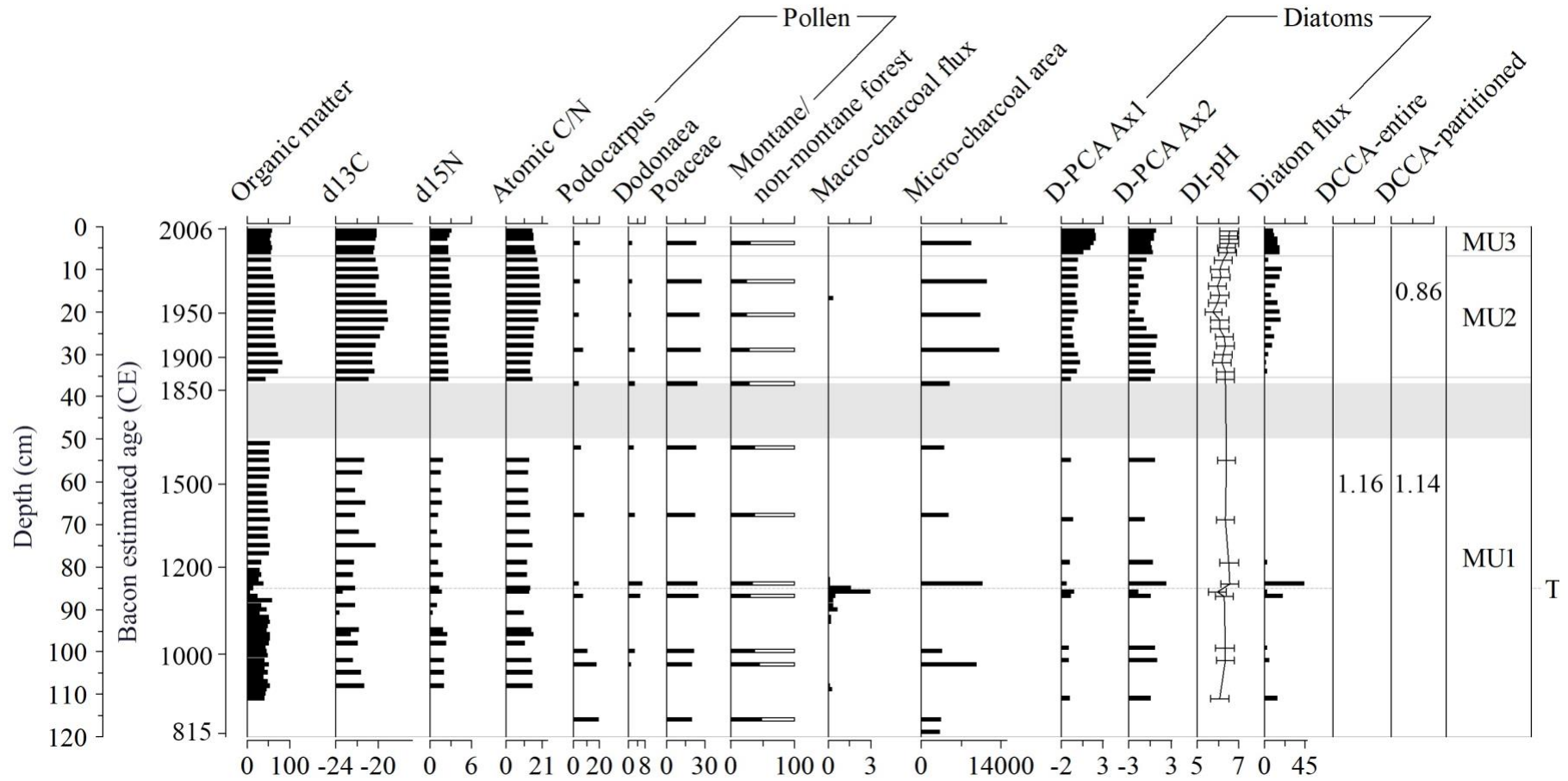
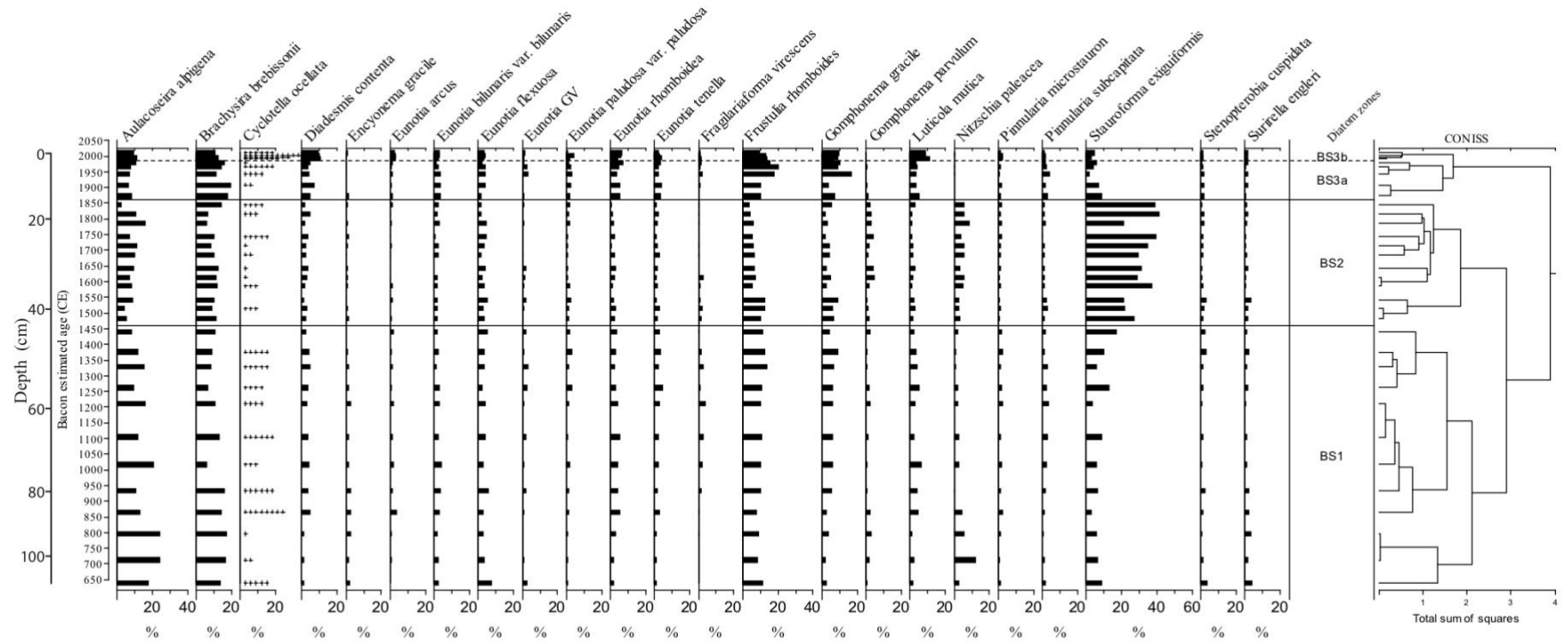


Figure 2: Selected sediment data for a) Bisoke core BIS3 and b) Muhavura cores MUH4-MUH2. Depth (cm) on the Y axis is depth beneath the lake bed. Estimated ages (expressed as Common Era, CE) are from BACON modelling based on AMS¹⁴C, ²¹⁰Pb and ¹³⁷Cs activities (Table S4) (Blaauw & Christen, 2011). Note that units for organic matter and pollen data = %, d15N and d13C represent, respectively, $\delta^{15}\text{N}$ and $\delta^{13}\text{C}$ (units = ‰), units for diatom flux are $\times 10^6$ valves $\text{cm}^{-2} \text{yr}^{-1}$. SCP = Spheroidal carbonaceous particles (flux = number of particles $\text{cm}^{-2} \text{yr}^{-1}$). Charcoal abundances are represented as Macro-charcoal (flux = $\text{mm}^2 \text{cm}^{-3} \text{yr}^{-1}$) and Micro-charcoal (area = $\text{cm}^2 \text{cm}^{-3}$). Results of data analysis are also

included in both a) and b) in the form of Principal components analysis (PCA) axes 1 and 2 diatom sample scores (axis 1 scores mainly reflect variations in the predominant diatoms, while axis 2 scores summarise variations in subdominant taxa) (D-PCA Ax1 and D-PCA Ax2), diatom-inferred pH (DI-pH) values, the results of Detrended Canonical Correspondence Analysis (DCCA) and diatom zone boundaries (BS1-BS3 and MU1-MU3) based on the results of constrained incremental sum of squares (CONISS) (Grimm, 1987) (see Figure 3). DCCA beta diversity results (standard deviation, SD, units) are provided for the full core (DCCA-entire), and for pre- and post-mid 19th century (DCCA-partitioned), and provide an estimate of compositional turnover. T = tephra. Note the missing sediment interval in b) between 1650 CE and 1860 CE (37cm to 50cm depth) and highlighted as grey-shading owing to non-retrieval of sediment during coring.

a)



b)

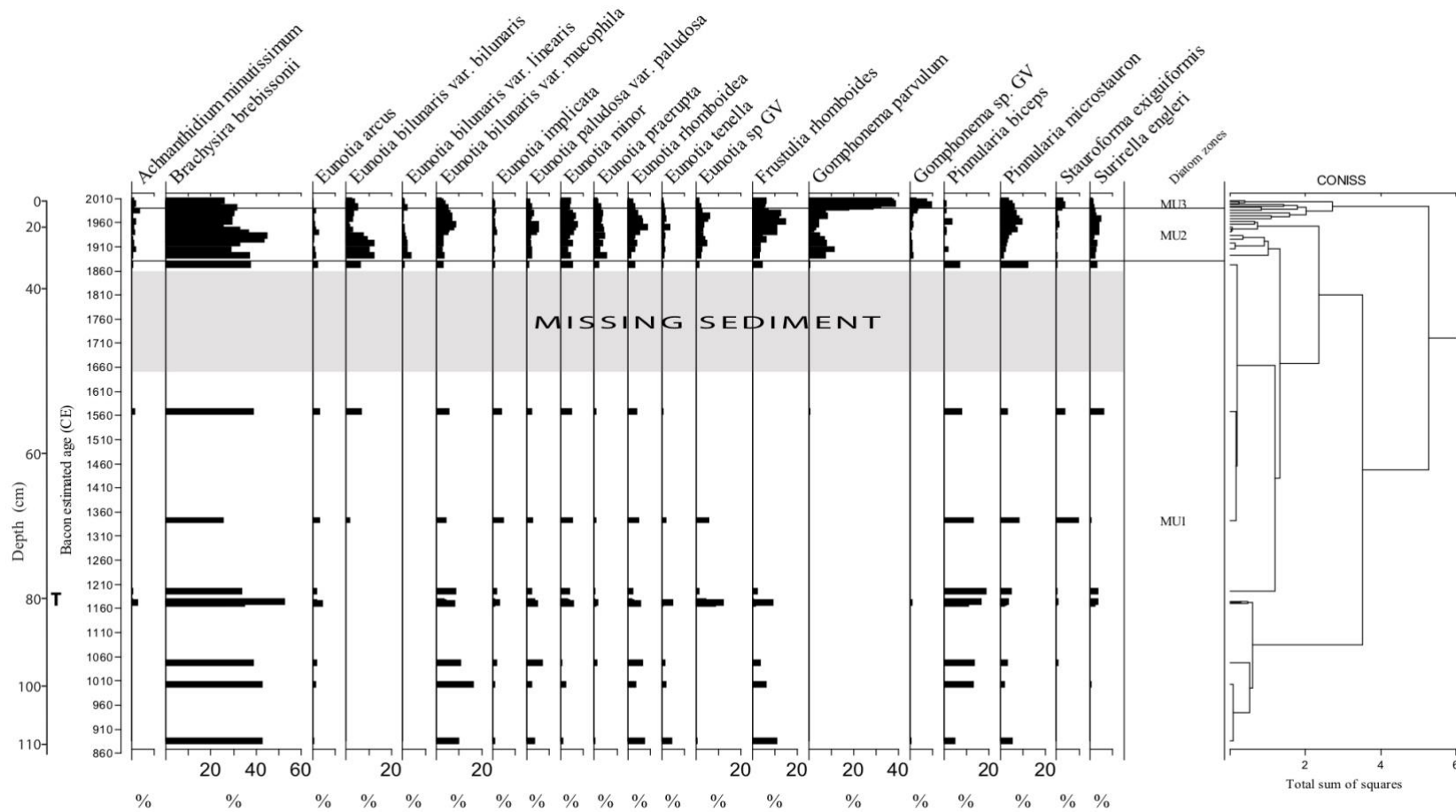


Figure 3: Variations in percent relative abundances of most common diatoms for a) BIS3 (minimum cut-off for inclusion $\geq 2\%$ in any one sample) and b) MUH4/MUH2 (minimum cut-off for inclusion $\geq 1\%$ in any one sample) cores, as well as for *Cyclotella ocellata* in (a). *C. ocellata* is found throughout BIS3, but reaches a peak of 2.5% in subzone BS3b. In b), relative abundances of *C. ocellata* (%s, levels marked with a “+”) are shown x 10. Estimated ages on the Y axis are from BACON modelling, shown as year Common Era (CE), and are based on

AMS¹⁴C, ²¹⁰Pb and ¹³⁷Cs activities (and see Table S4). X axis is % abundance. GV = Girdle View. Also shown are the results of constrained incremental sum of squares (CONISS) generated along with the Figure using the programme TILIA 2.0-41 (Grimm, 1987). Note the missing sediment interval in b) between 1650 CE and 1860 CE (37cm to 50cm depth) owing to non-retrieval of sediment during coring. T = tephra.

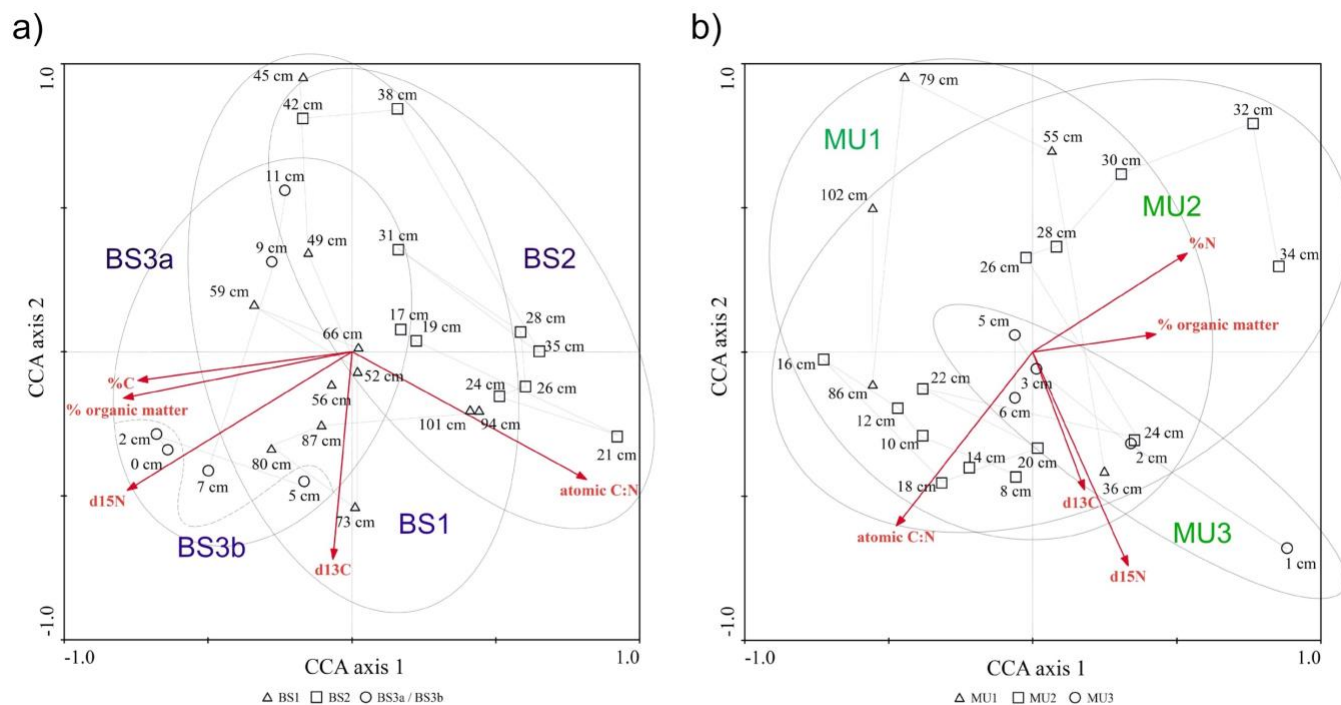
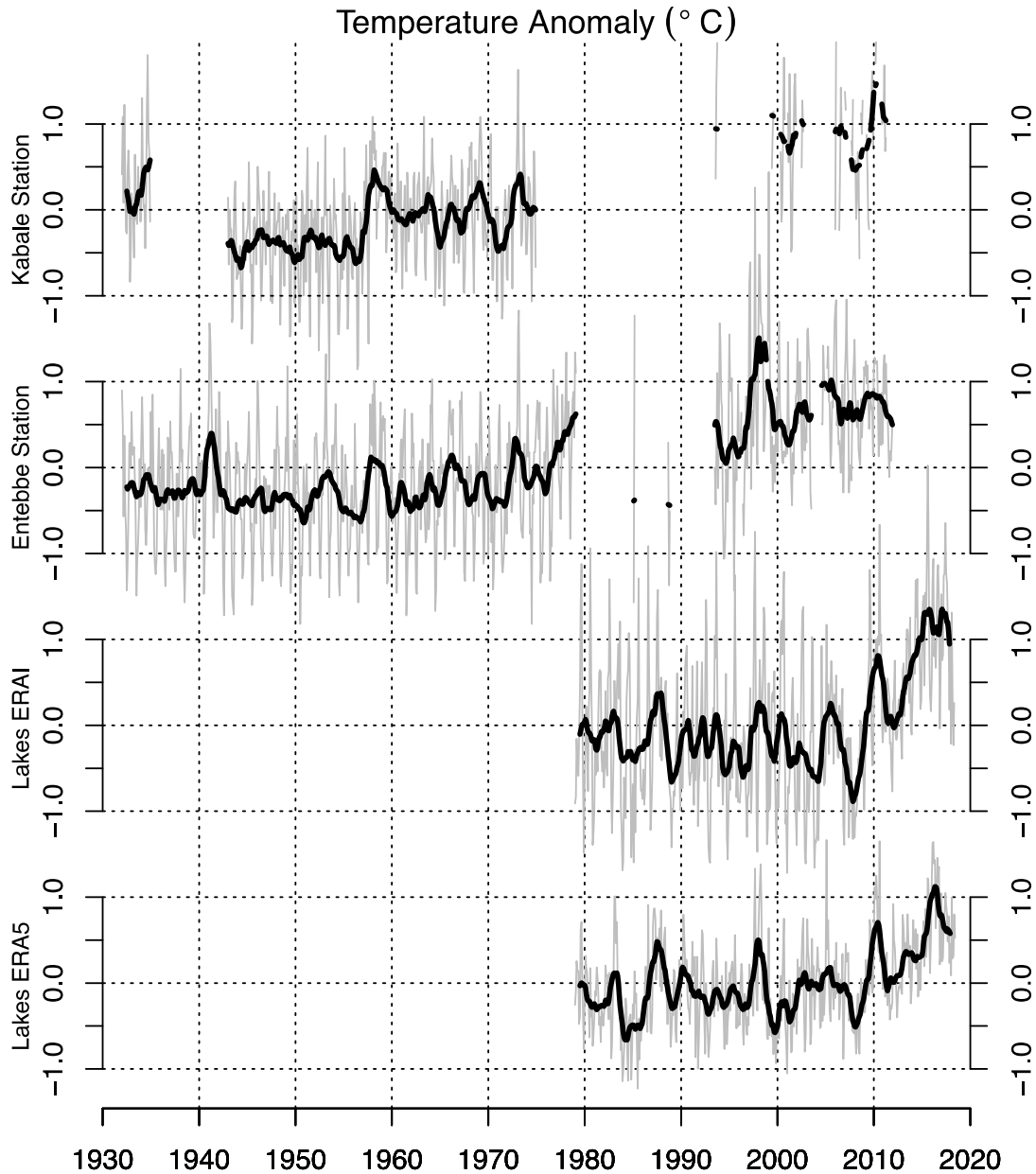


Figure 4: Results of Constrained Correspondence Analysis (CCA) using CANOCO 4.5 (ter Braak and Šmilauer, 2002) for diatom sediment sample data from a) Bisoke core BIS3 [27 sample levels included] and b) Muhavura cores MUH4/MUH2 [24 sample levels included]. Only diatom taxa that attained a level of >1% in at least one sample were included, along with selected environmental proxy data (% organic matter, % Total Nitrogen [TN], %Total Organic Carbon [TOC], atomic C:N, $\delta^{13}\text{C}$ (d13C) and $\delta^{15}\text{N}$ (d15N)). Diatom zones are shown. Stratigraphically contiguous samples are joined by a line. Note that %N and %C were excluded from, respectively a) BIS3 and b) MUH4/MUH2. See Table S5 for information on eigenvalues and explained variation.

2
3

4 **Figure 5:** Panels are described from the uppermost down. Monthly average temperature
 5 anomalies calculated with respect to series mean recorded at Kabale station, western Uganda,
 6 c. 30 km to the east of Mt. Muhavura with de-seasonalized trend (bold line) calculated using
 7 the zoo package of the R software; same for Entebbe station, central Uganda, on the northern
 8 shoreline of Lake Victoria, and with the most complete available record for the 20th century
 9 for a meteorological station close to the study area; the two lowermost panels show European
 10 Centre for Medium-Range Weather Forecasts (ECMWF) ERA-Interim (ERA-Interim, Dee et al.,
 11 2011) and ERA5 reanalysis monthly average temperature anomalies for the respective 75km
 12 and 35 km grid-cells that contain Bisoke and Muhavura lakes, with de-seasonalized trend
 13 shown (bold line). Note the significant gaps in the record and that the more complete record
 14 from Entebbe indicates c. 0.8-1.0 °C of warming since the 1930s.

15 **REFERENCES**

- 16 Abarca, N., Jahn, R., Zimmermann, J. & Enke, N. (2014) Does the cosmopolitan diatom
17 *Gomphonema parvulum* (Kützing) Kützing have a biogeography? *PLoS ONE*, 9: e86885
- 18 Abell, J.M., Özkundakci, D., Hamilton, D.P. & Jones, J.R. (2012) Latitudinal variation in
19 nutrient stoichiometry and chlorophyll-nutrient relationships in lakes: A global study.
20 *Fundamental and Applied Limnology / Archiv für Hydrobiologie*, 181, 1–14.
- 21 Alin, S.R. & Cohen, A.S. (2003) Lake-level history of Lake Tanganyika, East Africa, for the
22 past 2500 years based on ostracod-inferred water-depth reconstruction. *Palaeogeography,*
23 *Palaeoclimatology, Palaeoecology*, 199, 31-49
- 24 Anderson, M.J. (2006) Distance-based tests for homogeneity of multivariate dispersions.
25 *Biometrics*, 62, 245-253
- 26 Appleby, P.G. (2001) Chronostratigraphic techniques in recent sediments. In: W.M. Last &
27 J.P. Smol (Eds.) *Tracking environmental change using lake sediments. Volume 1: Basin*
28 *analysis, coring, and chronological techniques* (pp. 171–203). Dordrecht, The Netherlands:
29 Kluwer Academic Publishers.
- 30 Appleby, P.G. & Oldfield, F. (1978) The calculation of ²¹⁰Pb dates assuming a constant rate
31 of supply of unsupported ²¹⁰Pb to the sediment. *Catena*, 5, 1–8.
- 32 Ayebare, S., Plumptre, A.J., Kujirakwinja, D. & Segan, D. (2018) Conservation of the
33 endemic species of the Albertine Rift under future climate change. *Biological Conservation*,
34 220, 67-75.
- 35 Balagizi, C. M., F. Darchambeau, S. Bouillon, M. M. Yalire, T. Lambert & Borges, A.V.
36 (2015) River geochemistry, chemical weathering, and atmospheric CO₂ consumption rates in
37 the Virunga Volcanic Province (East Africa). *Geochemistry. Geophysics, Geosystems*, 16,
38 doi:10.1002/ 2015GC005999.

39 Baselega, A. & Orme, D.L. (2012) betapart: an R package for the study of beta diversity.
40 *Methods in Ecology and Evolution* 3, 808-812.

41 Battarbee, R.W., Jones, V.J., Flower, R.J., Cameron, N.G., Bennion, H., Carvalho, L., &
42 Juggins, S. (2001) Diatoms. In: J.P. Smol, H.J.B. Birks & W.M. Last (Eds.) *Tracking*
43 *environmental change using lake sediments. Volume 3: Terrestrial, algal, and siliceous*
44 *indicators* (pp. 155–205). Dordrecht, The Netherlands: Kluwer Academic Publishers.

45 Battarbee, R.W., Morley, D., Bennion, H., Simpson, G.L., Hughes, M. & Bauere, V. (2011) A
46 palaeolimnological meta-database for assessing the ecological status of lakes. *Journal of*
47 *Paleolimnology*, 45, 405-414

48 Bauters, M., Drake, T.W., Verbeeck, H., Bodé, S., Hervé-Fernández, P., Zito, P., ... Boeckx,
49 P. (2018) High fire-derived nitrogen deposition on central African forests. *Proceedings of the*
50 *National Academy of Sciences of the United States of America*, 115, 549-554

51 Bellinger, B.J., Cocquyt, C. & O'Reilly, C.M. (2006) Benthic diatoms as indicators of
52 eutrophication in tropical streams. *Hydrobiologia*, 573, 75–87.

53 Benedict, K.B., Prenni, A.J., Carrico, C.M., Sullivan, A.P., Schichtel, B.A. & Collett Jr., J.L.
54 (2017) Enhanced concentrations of reactive nitrogen species in wildfire smoke. *Atmospheric*
55 *environment*, 148, 8-15.

56 Bennett, K.D. (1996) Determination of the number of zones in a biostratigraphical sequence.
57 *New Phytologist*, 132, 155–170.

58 Bennett, K.D. & Willis, K.J. (2001). Pollen. J.P. Smol, H.J.B. Birks & W.M. Last (Eds.)
59 *Tracking environmental change using lake sediments. Volume 3: Terrestrial, algal, and*
60 *siliceous indicators* (pp. 5–32). Dordrecht, The Netherlands: Kluwer Academic Publishers.

61 Bere, T. & Tundisi, J.G. (2011) Influence of land-use patterns on benthic diatom communities
62 and water quality in the tropical Monjolinho hydrological basin, São Carlos-SP, Brazil. *Water*
63 *SA*, 37, 93-102

64 Birks, H.J.B. (1995) Quantitative palaeoenvironmental reconstructions. In: D. Maddy & J.S.
65 Brew (Eds.) *Statistical modelling of Quaternary science data* (pp 161–254). Cambridge:
66 Quaternary Research Association.

67 Birks, H.J.B. (2007) Estimating the amount of compositional change in late-Quaternary
68 pollen-stratigraphical data. *Vegetation History and Archaeobotany*, 16: 197-202.

69 Blaauw M and Christen JA. (2011) Flexible paleoclimate age-depth models using an
70 autoregressive gamma process. *Bayesian Analysis*, 6, 457-474.

71 Burgess, N.D., Balmford, A., Cordeiro, N.J., Fjeldså, J., Küper, W., Rahbek, C., ... Williams,
72 P.H. (2007) Correlations among species distributions, human density and human
73 infrastructure across the high biodiversity tropical mountains of Africa. *Biological*
74 *Conservation*, 134, 164–177.

75 Buytaert, W., Cuesta-Camacho, F. & Tobón, C. (2011) Potential impacts of climate change on
76 the environmental services of humid tropical alpine regions. *Global Ecology &*
77 *Biogeography*, 20, 19–33

78 Cárate-Tandalla, D., Camenzind, T., Leuschner, C. & Homeier, J. (2018) Contrasting species
79 responses to continued nitrogen and phosphorus addition in tropical montane forest tree
80 seedlings. *Biotropica*, 50, 234-245.

81 Catalan, J., Pla-Rabés, S., Wolfe, A.P., Smol, J.P., Rühland, K.M., ... Renberg, I. (2013)
82 Global change revealed by palaeolimnological records from remote lakes: a review. *Journal*
83 *of Paleolimnology*, 49, 513–535.

84 Cavalli-Sforza, L.L. & Edwards, A.W.F. (1967) Phylogenetic analysis: models and estimation
85 procedures. *Evolution*, 21, 550–570.

86 Chambers, J.W. & Cameron, N.G. (2001) A rod-less piston corer for lake sediments; an
87 improved, rope-operated percussion corer. *Journal of Paleolimnology*, 25, 117–122.

88 Cocquyt, C. (1998) *Diatoms from the northern basin of Lake Tanganyika*. Berlin: J. Cramer.

89 Cocquyt, C. & Jahn, R. (2007) *Surirella Engleri* O. Müller: A study of its original
90 infraspecific types, variability and distribution. *Diatom Research*, 22, 1–16.

91 Cohen, A.S., Gergurich, E.L., Kraemer, B.M., McGlue, M.M., McIntyre, P.B., Russell, J.M.,
92 ... Swarzenski, P.W. (2016) Climate warming reduces fish production and benthic habitat in
93 Lake Tanganyika, one of the most biodiverse freshwater ecosystems. *Proceedings of the*
94 *National Academy of Sciences*, 113, 9563-9568.

95 Cohen, A.S., Palacios-Fest, M.R., Msaky, E.S., Alin, S.R., McKee, B., ... Lezzar, K.E. (2005)
96 Paleolimnological investigations of anthropogenic environmental change in Lake Tanganyika:
97 IX. Summary of paleorecords of environmental change and catchment deforestation at Lake
98 Tanganyika and impacts on the Lake Tanganyika ecosystem. *Journal of Paleolimnology*, 34,
99 125-145.

100 Colombaroli, D., Ssemmanda, I., Gelorini, V. & Verschuren, D. (2014) Contrasting long-term
101 records of biomass burning in wet and dry savannas of equatorial East Africa. *Global Change*
102 *Biology*, 20, 2903-2914.

103 Conedera, M., Tinner, W., Neff, C., Meurer, M., Dickens, A.F. & Krebs, P. (2009)
104 Reconstructing past fire regimes: methods, applications, and relevance to fire management
105 and conservation. *Quaternary Science Reviews*, 28, 555–576.

106 Dalton, A.S., Patterson, R.T., Roe, H.M., Macumber, A.L., Swindles, G.T. ... Falck, H.
107 (2018) Late Holocene climatic variability in Subarctic Canada: Insights from a high-
108 resolution lake record from the central Northwest Territories. *PLoS ONE*, 13, e0199872

109 Davidson, T.A., Bennion, H., Reid, M., Sayer, C.D. & Whitmore, T.J. (2018) Towards better
110 integration of ecology in palaeoecology: from proxies to indicators, from inference to
111 understanding. *Journal of Paleolimnology*, 60, 109-116.

112 Dee, D.P., Uppala, S.M., Simmons, A.J., Berrisford, P., Poli, P., Kobayashi, S., ... Vitart, F.
113 (2011). The ERA-Interim reanalysis: confirmation and performance of the data assimilation
114 system. *Quarterly Journal of the Royal Meteorological Society*, 137, 553-597

115 Dornelas, M., Gotelli, N.J., McGill, B., Shimadzu, H., Moyes, F., ... Magurran, A.E. (2014)
116 Assemblage time series reveal biodiversity change but not systematic loss. *Science*, 296-299.

117 Felix, J.D., Elliott, E.M., Gish, T., McConnell, L. & Shaw, S. (2013) Characterizing the
118 isotopic composition of atmospheric ammonia emission sources using passive samplers and a
119 combined oxidation-bacterial denitrifier isotope ratio mass spectrometer method. *Rapid*
120 *Communication Mass Spectrometry*, 27, 2239-2246.

121 Felix, J.D., Elliott, E.M. & Shaw, S.L. (2012) Nitrogen isotopic composition of coal-fired
122 power plant NO_x: influence of emission controls and implications for global emission
123 inventories. *Environmental Science and Technology*, 46, 3528-3535.

124 Fowler, D., Coyle, M., Skiba, U., Sutton, M.A., Cape, J.N., Reis, S., ... Voss, M. (2013) The
125 global nitrogen cycle in the twenty-first century. *Philosophical Transactions of the Royal*
126 *Society B: Biological Sciences*, 368, 20130164.

127 Fritz, S.C., Benito, X., Steinitz-Kannan, M. (2019) Long-term and regional perspectives on
128 recent changes in lacustrine diatom communities in the tropical Andes. *Journal of*
129 *Paleolimnology*, 61, 252-262

130 Galy-Lacaux, C. & Delon, C. (2014) Nitrogen emission and deposition budget in West and
131 Central Africa. *Environmental Research Letters*, 9, 125002

132 Gasse, F. (1986) *East African diatoms: Taxonomy, ecological distribution*. Stuttgart: Cramer.

133 Gell, P.A., Sluiter, I.R & Fluin, J. (2002) Seasonal and interannual variations in diatom
134 assemblages in Murray River connected wetlands in north-west Victoria, Australia. *Marine*
135 *and Freshwater Research*, 53, 981-992.

136 Grimm, E.C. (1987) CONISS: a fortran 77 programme for stratigraphically constrained
137 cluster analysis by the method of incremental sum of squares. *Computers and Geosciences*,
138 13, 13–35.

139 Gütlein, A., Zistl-Schlingmann, M., Becker, J.N., Cornejo, N.S., Detsch, F., Dannenmann, M,
140 ... Kiese, R. (2017) Nitrogen turnover and greenhouse gas emissions in a tropical alpine
141 ecosystem, Mt. Kilimanjaro, Tanzania. *Plant Soil*, 411 243-259.

142 Hausmann, S., Charles, D.F., Gerritsen, J. & Belton, T.J. (2016) A diatom-based biological
143 condition gradient (BCG) approach for assessing impairment and developing nutrient criteria
144 for streams. *Science of the Total Environment*, 15, 914-927.

145 Heard, A.M., Sickman, J.O., Rose, N.L., Bennett, D.M., Lucero, D.M., Melack, J.M. &
146 Curtis, J.H. (2014) 20th Century atmospheric deposition and acidification trends in lakes of the
147 Sierra Nevada, California, USA. *Environmental Science and Technology*, 48, 10054-10061

148 Hedberg, O. (1964) Features of Afroalpine plant ecology. *Acta phytogeographica Suecica*,
149 49: 1-144

150 Heiri, O., Lotter, A.F. & Lemcke, G. (2001) Loss on ignition as a method for estimating
151 organic and carbonate content in sediments: reproducibility and comparability of results.
152 *Journal of Paleolimnology*, 25, 101–110.

153 Hobbs, W.O., Telford, R.J., Birks, H.J.B., Saros, J.E., Hazewinkel, R.R.O., Perren, B.B. ...
154 Wolfe, A.P. (2010) Quantifying recent ecological changes in remote lakes of North America
155 and Greenland using sediment diatom assemblages. *PLoS ONE*, 5, e10026

156 Hochleithner, S. (2017) Beyond contesting limits: land, access and resistance at the Virunga
157 National Park. *Conservation and Society*, 15, 100-110.

158 Holmgren, S.U., Ljung, K. & Björck, S. (2012) Late Holocene environmental history on
159 Tristan da Cunha, South Atlantic, based on diatom floristic changes and geochemistry in
160 sediments of a volcanic crater lake. *Journal of Paleolimnology*, 47, 221-232

161 Holtgrieve, G.W., Schindler, D.E., Hobbs, W.O., Leavitt, P.R., Ward, E.J., Bunting, L., ...
162 Wolfe, A.P. (2011) A coherent signature of anthropogenic nitrogen deposition to remote
163 watersheds of the northern hemisphere. *Science*, 334, 1545–1548.

164 Hu, Z., Anderson, N.J., Yang, X. & McGowan, S. (2014) Catchment-mediated atmospheric
165 nitrogen deposition drives ecological change in two alpine lakes in SE Tibet. *Global Change*
166 *Biology*, 20, 1614-1628.

167 Jewson, D.H. (1992) Size reduction, reproductive strategy and the life cycle of a centric
168 diatom. *Philosophical Transactions of the Royal Society*, B, 335:191–213

169 Jolly, D., Taylor, D., Marchant, R, Hamilton, A., Bonnefille, R., ... Riollet, G. (1997)
170 Vegetation dynamics in central Africa since 18,000 yr BP: pollen records from the
171 interlacustrine highlands of Burundi, Rwanda and western Uganda. *Journal of Biogeography*,
172 24, 492-512.

173 Kawashima, H. & Kurahashi, T. (2011) Inorganic ion and nitrogen isotopic compositions of
174 atmospheric aerosols at Yurihonjo, Japan: implications for nitrogen sources. *Atmospheric*
175 *Environment*, 45, 6309-6316.

176 Kilroy, C., Biggs, B.J.F., Vyverman, W. & Broady, P.A. (2006) Benthic diatom communities
177 in subalpine pools in New Zealand: relationships to environmental variables. *Hydrobiologia*,
178 561, 95-110.

179 Krammer, K. (1992) *Pinnularia: Eine Monographie der europäischen Taxa*. Berlin: Cramer.

180 Krammer, K. & Lange-Bertalot, H. (1986-1991) *Susswasserflora von Mitteleuropa*
181 *Bacillariophyceae, Teil 2-4*. Stuttgart: Gustav Fisher.

182 Lange-Bertalot, H. & Moser, G. (1994) *Brachysira: Monographie der Gattung*. Berlin:
183 Cramer.

184 Legendre, P. & Birks, H.J.B. (2012). From Classical to Canonical Ordination. In: H.J.B. Birks
185 et al. (Eds.), *Tracking Environmental Change Using Lake Sediments*, Developments in
186 paleoenvironmental Research 5. (pp 201-248) Springer Science + Business Media B.V

187 Litchman, E., Klausmeier, C.A., Miller, J.R., Schofield, O.M. & Falkowski, P.G. (2006)
188 Multi-nutrient, multi-group model of present and future oceanic phytoplankton communities.
189 *Biogeoscience*, 3, 585–606

190 Littke, R. (1985) Deposition, Diagenesis and Weathering of Organic Matter-Rich Sediments.
191 *Lecture Notes in Earth Sciences*. Volume 47, Springer, Berlin.

192 Mann, M.E., Zhang, Z., Rutherford, S., Bradley, R.S. Hughes, M.K., Shinwell, D., ... Ni, F.
193 (2009) Global signature and dynamical origins of the Little Ice Age and Medieval Climate
194 Anomaly. *Science*, 326, 1256-1260

195 McGill, B.J., Dornelas, M., Gotelli, N.J. & Magurran, A.E. (2015) Fifteen forms of
196 biodiversity trend in the Anthropocene. *Trends in Ecology & Evolution*, 30, 104-113

197 McGlynn, G., Mooney, S. & Taylor, D. (2013) Palaeoecological evidence for Holocene
198 environmental change from the Virunga volcanoes in the Albertine Rift, central Africa.
199 *Quaternary Science Reviews*, 61, 32–46.

200 Meyers, P.A. (2003) Applications of organic geochemistry to paleolimnological
201 reconstructions: a summary of examples from the Laurentian Great Lakes. *Organic*
202 *Geochemistry*, 34, 261-289.

203 Meyers, P.A. & Lallier-Vergès, E. (1999) Lacustrine sedimentary organic matter records of
204 Late Quaternary paleoclimates. *Journal of Paleolimnology*, 21, 345-372

205 Michelutti, N., Wolfe, A.P., Cooke, C.A., Hobbsm W.O., Vuille, M. & Smol, J.P. (2015)
206 Climate change forces new ecological states in tropical Andean lakes. *PLoS ONE* 10:
207 e0115338

208 Mills, K. & Ryves, D. (2012) Diatom-based models for inferring past water chemistry in
209 western Ugandan crater lakes, *Journal of Paleolimnology*, 48, 383-399.

210 Mills, K, Ryves, D.B., Anderson, N.J., Bryant, C.L. & Tyler, J.J. (2014) Expressions of
211 climate perturbations in western Ugandan crater lake sediment records during the last 1000
212 years. *Climates of the Past*, 10, 1581-1601

213 Mittermeier, R.A., Turner, W.R., Larsen, F.W., Brooks, T.M. & Gascon, C. (2011) Global
214 biodiversity conservation: the critical role of hotspots. In: F.E. Zachos & J.C. Habel (Eds.)
215 *Biodiversity hotspots* (pp 3–22). Heidelberg, Germany: Springer-Verlag.

216 Monchamp, M-E., Spaak, P., Domaizon, I., Dubois, N., Bouffard, D. & Pomati, F. (2018)
217 Homogenization of lake cyanobacterial communities over a century of climate change and
218 eutrophication. *Nature Ecology and Evolution*, 2, 317-324

219 Montoya-Moreno, Y. & Aguirre-Ramírez, N. (2013) Knowledge to ecological preferences in
220 tropical epiphytic algae to use with eutrophication indicators. *Journal of Environmental*
221 *Protection*, 4, 27-35.

222 Mooney, S.D. & Tinner, W. (2011) The analysis of charcoal in peat and organic sediments.
223 *Mires and Peat*, 7, 1–18.

224 Moritz, C. & Agudo, R. (2013) The future of species under climate change: resilience or
225 decline? *Science*, 341, 504-508.

226 MRI (Mountain Research Initiative EDW Working Group) (2015) Elevation-dependent
227 warming in mountain regions of the world. *Nature Climate Change*, 5, 424–430.

228 Nash, D.J., Gijss, D.C., Chase, B.M., Verschuren, D., Nicholson, S.E., Shanahan, T.M., ...
229 Grab, S.W. (2016) African hydroclimatic variability during the last 2000 years. *Quaternary*
230 *Science Reviews*, 154, 1-22

231 Nicholson, S.E., Funk, C., Fink, A.H. (2018) Rainfall over the African continent from the 19th
232 through the 21st century. *Global and Planetary Change*, 165, 114-127

233 O'Reilly, C. M., Sharma, S., Gray, D.K., Hampton, S.E., Read, J.S., Rowley, R.J., ... Zhang,
234 G. (2015) Rapid and highly variable warming of lake surface waters around the globe.
235 *Geophysical Research Letters*, 42, 10773-10781

236 Panizzo, V.N., Mackay, A.W., Ssemmanda, I., Taylor, R., Rose, N. & Leng, M.J. (2008). A
237 140-year record of recent changes in aquatic productivity in a remote, tropical alpine lake in
238 the Rwenzori Mountain National Park, Uganda. *Journal of Paleolimnology*, 40, 325-338.

239 Pérez, N.M., Hernández, P.A., Padilla, G., Nolasco, D., Barrancos, J., Melian, G. ... Ibarra,
240 M. (2011) Global CO₂ emission from volcanic lakes. *Geology*, 39, 235-238.

241 Pla, S., Monteith, D.T., Flower, R. J., Rose, N.L. (2009) The recent palaeolimnology of a
242 remote Scottish loch with special reference to the relative impacts of regional warming and
243 atmospheric contamination. *Freshwater Biology*, 54, 505-523.

244 Plumptre, A.J., Davenport, T.R.B., Behangana, M., Kityo, R., Eilu, G., Ssegawa, P., ...
245 Moyer, D., (2007) The biodiversity of the Albertine rift. *Biological Conservation*, 134, 178–
246 194.

247 Ponce-Reyes, R., Plumptre, A.J., Segan, D., Ayebare, S., Fuller, R.A., Possingham, H.P. &
248 Watson, J.E.M. (2017). Forecasting ecosystem responses to climate change across Africa's
249 Albertine Rift. *Biological Conservation*, 209, 464-472.

250 Ptacnik, R., Diehl, S. & Berger, S. (2003) Performance of sinking and nonsinking
251 phytoplankton taxa in a gradient of mixing depths. *Limnology & Oceanography*, 48, 1903–
252 1912

253 Reimer, P.J., Bard, E., Bayliss, A., Beck, J.W., Blackwell, P.G., Bronk Ramsey, C., ... van
254 der Plicht, J. (2013) IntCal13 and Marine13 radiocarbon age calibration curves, 0-50,000
255 years cal BP. *Radiocarbon*, 55, 1869-1887

256 Robbins, M.M., Gray, M., Fawcett, K.A., Nutter, F.B., Uwingeli, P., Mburanumwe, I.,
257 ...Robbins, A.M.. (2011) Extreme conservation leads to recovery of the Virunga mountain
258 gorillas. *PLoS ONE*, 6, e19788.

259 Rose, N. L. (1994). A note on further refinements to a procedure for the extraction of
260 carbonaceous fly-ash particles from sediments. *Journal of Paleolimnology*, 11, 201-204.

261 Rose, N. L. (2008). Quality control in the analysis of lake sediments for spheroidal
262 carbonaceous particles. *Limnology and Oceanography: Methods*, 6, 172-179.

263 Rose, N.L., Harlock, S. & Appleby, P.G. (1999) The spatial and temporal distributions of
264 spheroidal carbonaceous fly-ash particles (SCP) in the sediment records of European
265 mountain lakes. *Water and Soil Pollution*, 113, 1-32.

266 Rose, N.L., Juggins, S., Watt, J. & Battarbee, R. (1994) Fuel-type characterisation of
267 spheroidal carbonaceous particles using surface chemistry. *Ambio*, 23, 296-299.

268 Rühland, K., Paterson, A.M. & Smol, J.P. (2008) Hemispheric-scale patterns of climate-
269 related shifts in planktonic diatoms from North American and European lakes. *Global Change*
270 *Biology*, 14, 2740–2754

271 Rühland, K.M., Paterson, A.M. & Smol, J.P. (2015) Lake diatom responses to warming:
272 reviewing the evidence. *Journal of Paleolimnology*, 54, 1-35

273 Russell, J.M., McCoy, S.J., Verschuren, D., Bessems, I. & Huang, Y. (2009) Human impacts,
274 climate change, and aquatic ecosystem response during the past 2000 yr at Lake Wandakara,
275 Uganda. *Quaternary Research*, 72, 315–324.

276 Russell, J.M., Verschuren, D. & Eggermont, H. (2007) Spatial complexity of ‘Little Ice Age’
277 climate in East Africa: sedimentary records from two crater lake basins in western Uganda.
278 *The Holocene*, 17, 183-193.

279 Salerno, J., Chapman, C.A., Diem, J.E., Dowhaniuk, N., Goldman, A., MacKenzie, C.A., ...
280 Hartter, J. (2018) Park isolation in anthropogenic landscapes: land change and livelihoods at
281 park boundaries in the African Albertine Rift. *Regional Environmental Change*, 18, 913-928.
282 Saros, J.E., Northington, R.M., Anderson, D.S. & Anderson, N.J. (2016) A whole-lake
283 experiment confirms a small centric diatom species as an indicator of changing lake thermal
284 structure. *Limnology and Oceanography Letters*, 1, 27-35
285 Smol, J.P., Wolfe, A.P., Birks, H.J.B., Douglas, M.S.V., Jones, V.J., Korhola, A. ...
286 Weckström, J. (2005) Climate-driven regime shifts in the biological communities of arctic
287 lakes. *Proceedings of the National Academy of Sciences of the United States of America*, 102,
288 4397-4402.
289 Soeprbowati, T.R., Suedy, W.W.A, Hadiyanto, Luis, A.A. & Gell, P. (2018) Diatom
290 assemblage in the 24cm upper sediment associated with human activities in Lake Warna
291 Dieng Plateau Indonesia. *Environmental Technology and Innovation*, 10, 314-323.
292 Spinage, C.A. (1972) The ecology and problems of the Volcano National Park, Rwanda.
293 *Biological Conservation*, 4, 194-204.
294 Steffen, W., Grinevald, J., Crutzen, P. & McNeill, J. (2011) The Anthropocene: conceptual
295 and historical perspectives. *Philosophical Transactions of the Royal Society A: Mathematical,*
296 *Physical and Engineering Sciences*, 369, 842-867
297 Steinbauer, M.J., Grytnes, J-A., Jurasinski, G., Kulonen, A., Lenoir, J., Pauli, H. ... Wipf, S.
298 (2018) Accelerated increase in plant species richness on mountain summits is linked to
299 warming. *Nature*, 556, 231-234
300 Talbot, M.R. (2001) Nitrogen isotopes in palaeolimnology. In: W.M. Last & J.P. Smol (Eds.)
301 *Tracking environmental change using lake sediments. Volume 2: Physical and geochemical*
302 *methods* (pp 401–439). Dordrecht, The Netherlands: Kluwer Academic Publishers.

303 Taylor, D., Marchant, R.A. & Robertshaw, P. (1999) A sediment-based history of medium
304 altitude forest in central Africa: a record from Kabata Swamp, Ndae volcanic field, Uganda.
305 *Journal of Ecology*, 87, 303-315.

306 Taylor, D., Robertshaw, P. & Marchant, R.A. (2000) Environmental change and political-
307 economic upheaval in precolonial western Uganda. *The Holocene*, 10, 527-536

308 Taylor, D.M. (1990) Late Quaternary pollen records from two Ugandan mires: evidence for
309 environmental changes in the Rukiga Highlands of southwest Uganda. *Palaeogeography*,
310 *Palaeoclimatology, Palaeoecology*, 80, 283-300.

311 ter Braak, C. J. F. (1986) Canonical correspondence analysis – a new eigenvector technique
312 for multivariate direct gradient analysis. *Ecology*, 67, 1167–1179.

313 ter Braak, C.J.F. & Prentice, I.C. (1988). A theory of gradient analysis. *Advances in*
314 *Ecological Research*, 18, 271-317.

315 ter Braak, C. J. F. & Šmilauer, P. (2002) *CANOCO reference manual and CanoDraw for*
316 *Windows user's guide: software for canonical community ordination (version 4.5)*. New
317 York: Microcomputer Power, Ithaca, pp. 352.

318 Tierney, J.E., Mayes, M.T., Meyer, N., Johnson, C., Swarzenski, P.W. Cohen, A.S. & Russell,
319 J.M. (2010) Late-twentieth-century warming in Lake Tanganyika unprecedented since AD
320 500. *Nature Geoscience*, 3, 422-425

321 Van der Werf, G.R. Randerson, J.T., Giglio, L., van Leeuwen, T.T., Chen, Y., Rogers, B.M.,
322 ... Kasibhatla, P.S. (2017) Global fire emissions estimates during 1997-2016. *Earth System*
323 *Science Data*, 9, 697-720.

324 Verschuren, D., Laird, K.R. & Cumming, B.F. (2000) Rainfall and drought in equatorial east
325 Africa during the past 1100 years. *Nature*, 403, 410-414.

326 Waddington, J.C.B. (1969) A stratigraphic record of the pollen influx to a lake in the Big
327 Woods of Minnesota. *Geological Society of America Special Paper*, 123, 263–282.

328 Wang, Y-L., Liu, X-Y., Song, W., Yang, W., Han, B., Dou, X-Y., ... Bai, Z-P. (2017) Source
329 apportionment of nitrogen in PM_{2.5} based on bulk $\delta^{15}\text{N}$ signatures and a Bayesian isotope
330 mixing model. *Tellus B: Chemical and Physical Meteorology*, 69, 1299-672

331 Waters, C.N., Zalasiewicz, J.A., Williams, M., Ellis, M.A. & Snelling, A.M. (2014) A
332 stratigraphical basis for the Anthropocene? In: C.N. Waters, J.A. Zalasiewicz, M. Williams,
333 M.A. Ellis & A.M. Snelling (Eds) A stratigraphical basis for the Anthropocene (pp 1-21).
334 Geological Society, London, Special Publications, 395.

335 Wengrat, S., Padial, A.A., Jeppesen, E., Davidson, T.A., Fontana, L., Costa-Böddeker, S. &
336 Bicudo, D.C. (2018) Paleolimnological records reveal biotic homogenization driven by
337 eutrophication in tropical reservoirs. *Journal of Paleolimnology*, 60, 299-309

338 Winder, M & Hunter, D.A. (2008) Temporal organization of phytoplankton communities
339 linked to physical forcing. *Oecologia*, 156, 179–192

340 Wilkinson, I.P., Poirier, C., Head, M.J., Sayer, C.D. & Tibby, J. (2014) Microbiotic signatures
341 of the Anthropocene in marginal marine and freshwater palaeoenvironments. In: C.N. Waters,
342 J.A. Zalasiewicz, M. Williams, M.A. Ellis & A.M. Snelling (Eds) A stratigraphical basis for
343 the Anthropocene (pp 185-219). Geological Society, London, Special Publications, 395.

344 Wood, D.A. & Scholz, C.A. (2017) Stratigraphic framework and lake level history of Lake
345 Kivu, East African Rift. *Journal of African Earth Sciences*, 134, 904-916

346 Yan, Y., Wang, L., Li, J., Li, J., Zou, Y., Zhang, J., ... Wan, X. (2018) Diatom response to
347 climatic warming over the last 200 years: A record from Gonghai Lake, North China.
348 *Palaeogeography, Palaeoclimatology, Palaeoecology*, 495, 48-59

349 Yang, Y., Stenger-Kovács, C., Padisák, J. & Pettersson, K. (2016) Effects of winter severity
350 on spring phytoplankton development in a temperate lake (Lake Erken, Sweden).
351 *Hydrobiologia*, 780, 47-57.

352 Zimmer, A., Meneses, R.I., Rabatel, A., Soruco, A., Dangles, O. & Antheleme, F. (2018)
353 Time lag between glacial retreat and upward migration alters tropical alpine communities.
354 *Perspectives in Plant Ecology, Evolution and Systematics*, 30, 89-102.

355 Zwiener, V.P., Lira-Noriega, A., Grady, C.J., Padial, A.A. & Vitule, J.R.S. (2018) Climate
356 change as a driver of biotic homogenization of woody plants in the Atlantic Forest. *Global*
357 *Ecology and Biogeography*, 27, 298-309.

358

359 **BIOSKETCH**

360 Gayle McGlynn is an Assistant Professor in the School of Natural Sciences, Trinity College,
361 University of Dublin. She holds a PhD in environmental change and its impacts in eastern
362 Africa. Gayle has carried out field-based research in Africa in Burundi, Kenya, Rwanda,
363 Tanzania, Uganda and Zambia. David Taylor is Provost's Chair and Professor of Tropical
364 Environmental Change in the Department of Geography at National University of Singapore.
365 A tropical palynologist by training, he has more than 35 years of research experience in
366 tropical Africa and Asia.

367

368 **AUTHOR CONTRIBUTIONS**

369 GMcG and DT were involved in all aspects of the paper and the research that underpins it,
370 including fieldwork. CD and JL were involved in part of the fieldwork. AT, NR, SM, WB,
371 ZT, XZ & KR provided data and/or helped with data analysis. All authors were involved in
372 writing the paper, led by DT.

373

374 **DATA ARCHIVING**

375 Research data referred to in this paper will be kept for a minimum of 10 years, according to
376 the Research Data Management Policy of the National University of Singapore.

377

378